UNIVERSIDAD DE CÓRDOBA

TESIS DOCTORAL

Estimación hidrológica del riesgo de sequía

Hydrological assessment of drought risk

Autora:

María del Pilar Jiménez Donaire

Directores:

Juan Vicente Giráldez Cervera

Tom Vanwalleghem

Programa de doctorado:

Dinámica de flujos biogeoquímicos y sus aplicaciones

Febrero 2021

TITULO: *Hydrological assessment of drought risk*

AUTOR: *María Pilar Jiménez Donaire*

© Edita: UCOPress. 2021
Campus de Rabanales
Ctra. Nacional IV, Km. 396 A
14071 Córdoba

https://www.uco.es/ucopress/index.php/es/
ucopress@uco.es

TÍTULO DE LA TESIS: Estimación hidrológica del riesgo de sequía

DOCTORANDO/A: María del Pilar Jiménez Donaire

INFORME RAZONADO DEL/DE LOS DIRECTOR/ES DE LA TESIS

(se hará mención a la evolución y desarrollo de la tesis, así como a trabajos y publicaciones derivados de la misma).

La doctoranda ha realizado un excelente trabajo, cumpliendo con satisfacción todos los objetivos propuestos y creemos además que ha desarrollado de forma satisfactoria su formación como doctora. Esta tesis ha resultado en la actualidad en tres publicaciones SCI y dos contribuciones a congresos internacionales.

Jiménez-Donaire, M. del P., Giráldez, J.V., Vanwalleghem, T., 2020. Evaluation of Drought Stress in Cereal through Probabilistic Modelling of Soil Moisture Dynamics. Water 12, 2592. https://doi.org/10.3390/w12092592

Jiménez-Donaire, M. del P., Giráldez, J.V., Vanwalleghem, T., 2020. Impact of Climate Change on Agricultural Droughts in Spain. Water 12, 3214. https://doi.org/10.3390/w12113214

Jiménez-Donaire, M. del P., Tarquis, A., Giráldez, J.V., 2020. Evaluation of a combined drought indicator and its potential for agricultural drought prediction in southern Spain. Natural Hazards and Earth System Sciences 20, 21–33. https://doi.org/10.5194/nhess-20-21-2020

Por todo ello, se autoriza la presentación de la tesis doctoral.

Córdoba, 16 de febrero de 2021

Firma del/de los director/es

GIRALDEZ CERVERA JUAN VICENTE - 31165788Y
Firmado digitalmente por GIRALDEZ CERVERA JUAN VICENTE - 31165788Y
Fecha: 2021.02.17 07:30:30 +01'00'

VANWALLEGHEM TOM S K - X7356177H
Firmado digitalmente por VANWALLEGHEM TOM S K - X7356177H
Fecha: 2021.02.16 23:06:37 +01'00'

Fdo.:_Juan Vicente Giráldez Cervera Fdo.: Tom Vanwalleghem

RESUMEN

La sequía agrometeorológica o agrícola es una de las más graves contingencias a la que se enfrenta la agricultura y por tanto la sociedad en su conjunto, ya que se define en términos de pérdida de cosecha provocando escasez de alimentos. A su vez, la sequía es la amenaza de origen natural que afecta a más personas en el conjunto del planeta. La mayoría de los estudios sobre sequía no cuantifican de manera fiable su efecto sobre la productividad agrícola ni abordan las consecuencias de las predicciones de cambio climático sobre la extensión y la intensidad de las sequías.
Una buena comprensión y el desarrollo de modelos adecuados de predicción de ocurrencia de sequías a escala tanto a corto como a medio plazo es esencial para una adecuada gestión de los recursos hídricos y de la producción agrícola. Asimismo, se pueden obtener importantes beneficios de mejorar la vigilancia y la predicción a largo plazo de las sequías, para lo que es fundamental tener en cuenta las proyecciones de escenarios de cambio climático.

En esta tesis se han aplicado por primera vez los indicadores de estrés de sequía estático y dinámico propuestos por Porporato, validándolos frente a datos observados de rendimiento de cultivos, para evaluar sequías agrícolas a escala local. Se identificaron correctamente los periodos de sequía ocurridos poniendo de manifiesto su gran utilidad y se demostró que ambos indicadores presentan mejores resultados que los indicadores tradicionales de sequía como el SPI-3. Se realizó un análisis de sensibilidad revelando el impacto de la profundidad del suelo en las variaciones espaciales de los indicadores, presentando una respuesta compleja en función de la precipitación anual.
En la tesis se propone un nuevo indicador combinado de sequía (ICS), que se evaluó a escala regional frente a datos observados de daños en cultivos de cereales en secano, identificando correctamente los eventos importantes de sequía acaecidos. Se ha diseñado un sistema de avisos de situaciones de sequía agrícola a partir del ICS basado en la combinación de sus componentes, que invita a poner en marcha las medidas oportunas para paliar los efectos de la sequía.
Por otro lado, se han modelado los efectos del cambio climático sobre los eventos de sequía a escala nacional hasta 2100, empleando el escenario de emisión RCP8.5. Se mostraron las ventajas, frente a otros indicadores, del empleo de los indicadores de estrés estático y dinámico, teniendo este último la ventaja respecto a otros indicadores de incluir, además de la intensidad, información sobre la duración media y la frecuencia de los eventos de sequía en un único indicador.

Los resultados obtenidos mostraron que los indicadores propuestos por Porporato identifican correctamente los periodos de sequía ocurridos en las zonas de estudio y presentan mejores resultados que los indicadores tradicionales de sequía.
Por otro lado, los resultados demostraron que el ICS propuesto presenta consistencia con los eventos de sequía agrícola ocurridos en la región de estudio y presenta potencial para servir como indicador de avisos de sequía agrícola futura además de proporcionar distintas ventajas respecto al uso de indicadores simples.
Por último, los resultados determinaron que tanto la severidad como la frecuencia y la intensidad de las sequías se verán incrementadas en el escenario RCP8.5 en nuestro país, en particular en el subperiodo 2071-2100.

INTRODUCTION

Drought is one of the major natural hazards affecting agricultural crop production and food security throughout history (Toonen et al., 2020) and in our own time (FAO, 2020a). The percentage of the planet affected by drought has more than doubled in the last 40 years and droughts have affected more people than any other natural hazard (FAO, 2020b). The UN estimates that a decade from now, up to 700 million people will be compelled to leave their homes because of water shortages ("End the drought in drought research," 2019). Mediterranean countries, like Spain, have historically been affected by a large variability in their rainfall regime and by droughts. However, Spinoni et al. (2017) have shown that drought events are not localized to these traditional hotspots and droughts are increasing all over Europe in the last decades. They analyzed tendencies from 1950 to 2015 and found an evolution towards drier conditions in Central Europe in spring, in the Mediterranean basin in summer and in Eastern Europe in fall. The importance of droughts will only increase as future climate change projections, with decreasing precipitation and increasing temperature (IPCC, 2014), draw a problematic outlook for agricultural production, with lower soil moisture, increasing demand for water, and diminishing water supplies. Schmidhuber and Tubiello (2007) analyze the potential impacts of climate change on food security and show how the problem is even wider than just agricultural production and will impact society profoundly. They highlight how climate change will affect four fundamental aspects of food security: (i) food production and availability, (ii) stability of food supplies, (iii) food utilization and (iv) food prices. Most studies have addressed the first aspect, but even so the extent and intensity of climate change predictions on droughts and agricultural productivity have not yet been reliably quantified. As these depend highly on the scenario, models and indicators used, there is an ongoing debate in the scientific community. In a European study by the Joint Research Center of the EU, Císcar-Martínez et al. (2018) project significant drying trends in the west of the Mediterranean region, while they expect wetting in Central and Eastern Europe. In contrast, Lu et al. (2019) predict large-scale drying and limited wetting globally for all climate change scenarios, and identify Europe and the Mediterranean as one of the main hotspots where the mean spatial extent of severe drought will increase.

Given the importance of droughts, a good understanding and development of adequate models for predicting drought occurrence at short and medium time scales is essential to manage water resources and agricultural production adequately. Additionally, agricultural insurance schemes and farmers can benefit from improved drought monitoring and prediction. Insurance policies, especially agricultural ones, are currently are short-term and pricing does not reflect climate change over the policy period, however insurers increasingly recognize the importance of taking into account climate change projections, and particularly the role insurance can play in climate change adaptation (Erhardt et al., 2019).

Consequently, with this in mind, it is pertinent to first define drought and select the scale under study, as these will strongly condition the monitoring and prediction tools that

are best suited. No universally accepted definition of drought exists as the complexity of the phenomenon inherently difficults an accurate description (Quiring, 2009). Slette et al. (2019), after a literature review, concluded that ecologists characterized drought in a wide variety of ways, for example reduced precipitation to reduced soil moisture or streamflow, but that only as few as 32% of the studies actually defined drought explicitly. Generally, four types are distinguished, following Wilhite and Glantz (1985), according to how the effects were noticed: (i) meteorological, due to the scarcity of rainfall; (ii) hydrological, detected by low streamflow; (iii) agricultural, when soil water is not sufficient to maintain a crop; and (iv) socioeconomic, when it affects the normal functioning of society. In this study, focus will be on agricultural drought, and its relation to crop yield.

A large number of indicators have been proposed to monitor and evaluate drought stress. A common classification of such indicators is made according to the drought type considered, i.e. precipitation and temperature-based indicators for meteorological drought, soil moisture and vegetation stress based-indicators for agricultural drought, streamflow or groundwater level for hydrological droughts and supply-demand or pricing for socio-economical drought, although the latter is much less frequent (Bachmair et al., 2016).

Two main meteorological drought indices are the Palmer Drought Severity Index (PDSI) and the the Standardized Precipitation Index (SPI). The first, PDSI was first published in 1965 by meteorologist Wayne Palmer (Keyantash and Dracup, 2002), and is based on precipitation and temperature, and is still widely used. In his original paper, Palmer (1965) specifically excludes agricultural and hydrological drought problems and focusses on meteorological drought. The most widely used and best known drought index is undoubtably the Standardized Precipitation Index (SPI) (Lloyd-Hughes and Saunders, 2002; Mckee et al., 1993). Vicente-Serrano et al. (2010) proposed a modified version of the SPI, the Standardised Precipitation-Evapotranspiration Index (SPEI), that has gained a lot of popularity in recent years since it also includes evapotranspiration in addition to precipitation, and therefore approximates better the water balance. The different drought indices are also subject to continuous improvement. For example, Hobbins et al. (2016) have modified the SPEI index by representing the potential evapotranspiration and the atmospheric evaporative demand on a proper physical basis, rather than on the air temperature as a proxy of it. Their evaporative demand drought index (EDDI) is a useful indicator of drought extent, as was shown by McEvoy et al. (2016) in the conterminous US. Figure 1 summarizes the number of papers published per year and total, using the three previously cited indices: SPI, PDSI and SPEI. For this figure, the search terms “drought” and the respective drought index were used in Web of Science. It can be seen that SPI is by far the most used drought index, although SPEI is gaining a lot of prevalence in recent years. The PDSI was the first drought index to appear in scientific literature, and has been used consistently used since, although it was never as widely used as SPI and SPEI. In addition, a significant increase in drought research can be observed in recent years, with around 70% of the papers published in the last 5 years.

Nonetheless, the drought indicators based on remote-sensing data of vegetation condition do not fit well in the previous classification of indicators according to drought type. This refers to indicators such as the widely used Normalized Differential Vegetation Index (NDVI), or Vegetation Condition Index (VCI), proposed by Kogan (1995) and based on NDVI. AghaKouchak et al. (2015) review the state-of-the-art with respect to these remote-sensing-based indicators and their potential. They indicate that the main limitation related to these indicators is the short length of record of many of the currently available satellite observations, often limited to a decade or less. On the other hand, they highlight the current and future possibility of development of composite drought indicators. Such composite or combined indicators, that combine traditional climate and satellite-based drought indices, have been proposed in a number of studies in recent years (Sepulcre-Canto et al., 2012). Keyantash and Dracup (2002) were among the first to propose such an approach. They called their index "Aggregate drought index", and it contained information on all physical forms of drought (meteorological, hydrological, and agricultural) through selection of variables that are related to each drought type. Such indicators could contribute significantly to produce a simple and more comprehensive picture of drought.

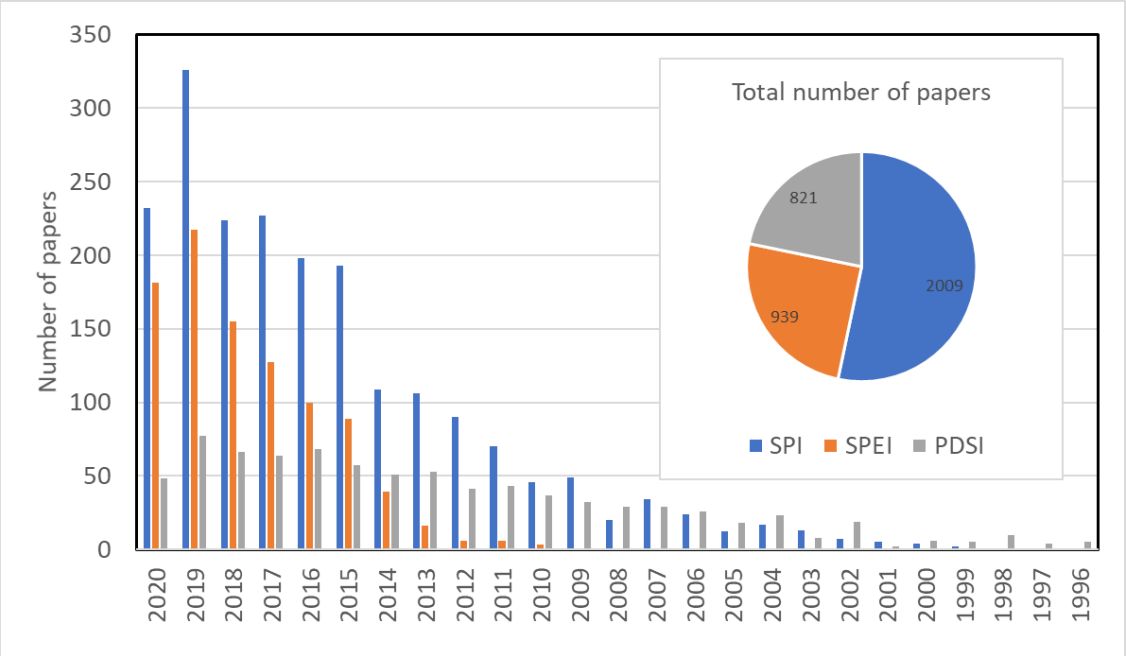

Figure 1. Number of papers using different drought indices, per year and total, according to Web of Science.

Purdy et al. (2019) flag an important problem with all these different indicators, which is that drought indicators are often designed following a top-down approach, as scientists traditionally design drought indicators with little input from the end users, resulting results in indicators that are sometimes not aligned with needs of stakeholders (Steinemann et al., 2015). They propose that important improvements can be made in the design of drought indicators from the perspective of product design. Despite stakeholders having many drought indicators to their disposal, they are unsure if any of them was suitable to support their operations. As a consequence, efforts have been

made to simplify and improve the user experience, and create a “general” drought indicator. Examples are the United States Drought Monitor (“United States Drought Monitor,” 2020) or the European Drought Observatory (JRC European Commission, 2020), that give a quick “snapshot” view of the drought situation at continental scale. However, according to Purdy et al. (2019) this “one-size-fits-all” approach may not fit any one stakeholder group well either. In a revision study, Bachmair et al. (2016) found 33 providers of operational drought monitoring, and, while they detected a lot of variability in the used indicators, they also report that the most recent trend leans towards using composite indicators. They also flag an important research gap, that the monitoring of impact of drought lacks systematization. Their review found 14 research papers assessing the relation of drought indicators to crop yield, 7 to remotely sensed vegetation stress, 6 to text-based data and 4 to other impact variables or several in parallel. These relatively low numbers indicate that more research effort needs to be done in the analysis of the relation between drought indicators and the impact of droughts, such as yield loss or crop damage.

The hypothesis behind this study is that drought research, and especially research into the impact of droughts on agricultural crop production, needs to be adapted to the specific temporal and spatial scale under study, that can range from local to regional to national, and from past to present to future. The different spatial scales are related to data inputs and decisions, as proposed by Purdy et al. (2019) as shown in Figure 2.

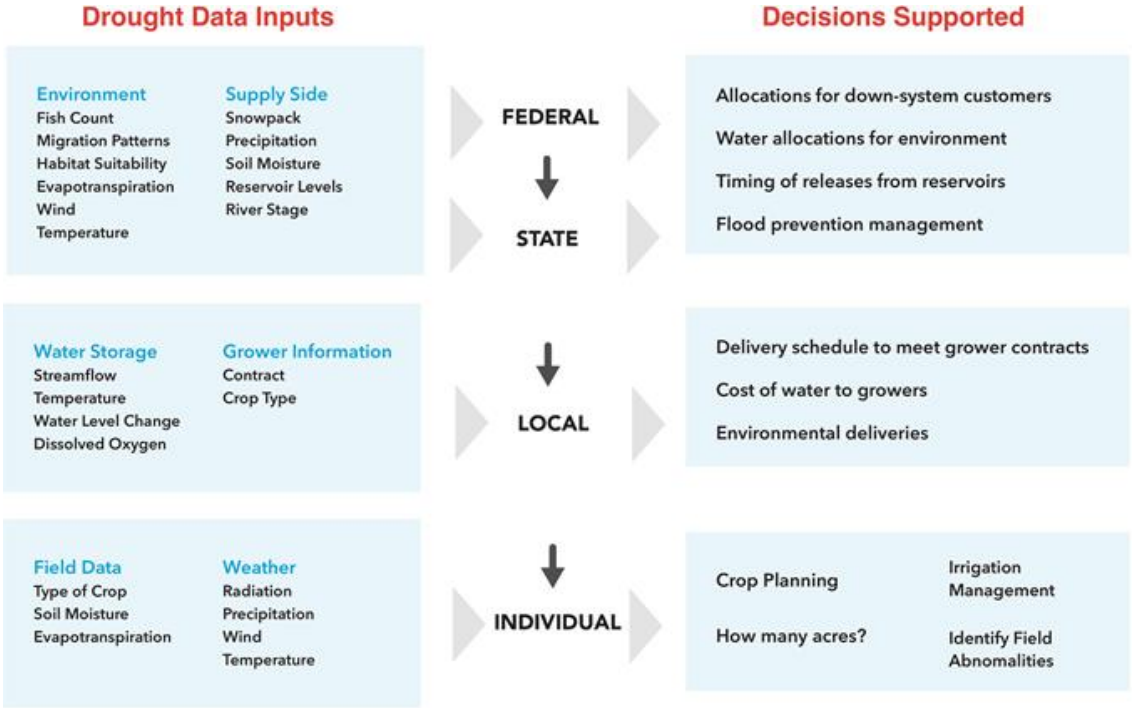

Figure 2. Data dependencies and decisions supported by different stakeholders at different spatial scales of interest (reproduced from Purdy et al. (2019))

The overall objective of this study is to improve the understanding and monitoring of agricultural droughts at different scales. For this purpose, new drought indicators have been proposed and tested at scales ranging from the local scale of Cordoba, to the regional scale of Andalusia, to the national scale of Spain.

This has allowed to address novel issues such as how external conditions that affect the relation between droughts and agricultural production at these scales, for instance soil properties or crop type. This has been discussed in more details in chapters 1 and 2, where the relation of the newly proposed drought indicators with yield and agricultural insurance data is analyzed. In chapter 3 an outlook into future drought predictions is given by incorporating global climate change predictions.

The present study is organized as follows, according to an increasing spatial scale and the time frame analyzed:

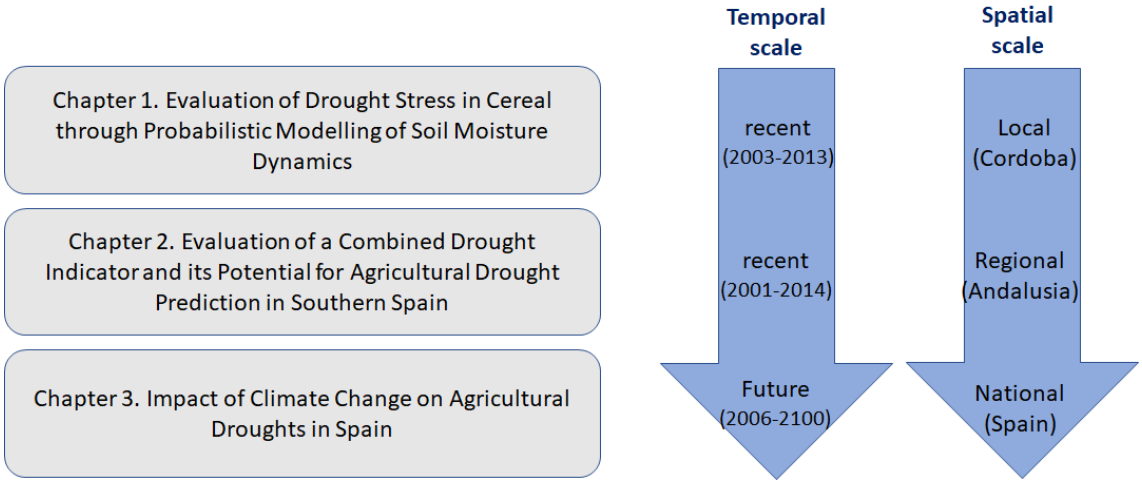

Figure 3. Organization of this study, and relation to temporal and spatial scales.

References

AghaKouchak, A., Farahmand, A., Melton, F.S., Teixeira, J., Anderson, M.C., Wardlow, B.D., Hain, C.R., 2015. Remote sensing of drought: Progress, challenges and opportunities. Rev. Geophys. 53, 452–480. https://doi.org/10.1002/2014RG000456

Bachmair, S., Stahl, K., Collins, K., Hannaford, J., Acreman, M., Svoboda, M., Knutson, C., Smith, K.H., Wall, N., Fuchs, B., Crossman, N.D., Overton, I.C., 2016. Drought indicators revisited: the need for a wider consideration of environment and society. WIREs Water 3, 516–536. https://doi.org/10.1002/wat2.1154

Ciscar Martinez, J.-C., Ruiz, D., Ramirez, A., Dosio, A., Toreti, A., Ceglar, A., Fumagalli, D., Dentener, F., Lecerf, R., Zucchini, A., Panarello, L., Niemeyer, S., Domínguez, I., Fellmann, T., Kitous, A., Després, J., Christodoulou, A., Demirel, H., Alfieri, L., Feyen, L., 2018. Climate impacts in Europe: final report of the JRC PESETA III project. https://doi.org/10.2760/93257

"End the drought in drought research," 2019. End the drought in drought research. Nature 573, 310–310. https://doi.org/10.1038/d41586-019-02782-3

Erhardt, R., Bell, J., Blanton, B., Nutter, F., Robinson, M., Smith, R., 2019. Stronger Climate Resilience with Insurance. Bull. Am. Meteorol. Soc. 100, 1549–1552. https://doi.org/10.1175/BAMS-D-19-0073.1

FAO, 2020a. The State of Food Security and Nutrition in the World 2020: Transforming food systems for affordable healthy diets, The State of Food Security and Nutrition in the World (SOFI). FAO, IFAD, UNICEF, WFP and WHO, Rome, Italy. https://doi.org/10.4060/ca9692enAlso Available in:Chinese Spanish Arabic French Russian

FAO, 2020b. Drought and Agriculture [WWW Document]. URL http://www.fao.org/land-water/water/drought/droughtandag/en/ (accessed 10.15.20).

Hobbins, M.T., Wood, A., McEvoy, D.J., Huntington, J.L., Morton, C., Anderson, M., Hain, C., 2016. The Evaporative Demand Drought Index. Part I: Linking Drought Evolution to Variations in Evaporative Demand. J. Hydrometeorol. 17, 1745–1761. https://doi.org/10.1175/JHM-D-15-0121.1

IPCC, 2014. Climate Change 2014: Synthesis Report. Contribution of Working Groups I, II and III to the Fifth Assessment Report of the Intergovernmental Panel on Climate Change [Core Writing Team, R.K. Pachauri and L.A. Meyer (eds.)]. Geneva, Switzerland.

JRC European Commission, 2020. European Drought Observatory [WWW Document]. URL https://edo.jrc.ec.europa.eu/edov2/php/index.php?id=1000 (accessed 10.23.20).

Keyantash, J., Dracup, J.A., 2002. The Quantification of Drought: An Evaluation of Drought Indices. Bull. Am. Meteorol. Soc. 83, 1167–1180. https://doi.org/10.1175/1520-0477-83.8.1167

Kogan, F.N., 1995. Application of vegetation index and brightness temperature for drought detection. Adv. Space Res. 15, (11)91-(11)100. doi: 0273-1177~95NO079-8

Lloyd-Hughes, B., Saunders, M.A., 2002. A drought climatology for Europe. Int. J. Climatol. 22, 1571–1592. https://doi.org/10.1002/joc.846

Lu, J., Carbone, G.J., Grego, J.M., 2019. Uncertainty and hotspots in 21st century projections of agricultural drought from CMIP5 models. Sci. Rep. 9, 4922. https://doi.org/10.1038/s41598-019-41196-z

McEvoy, D.J., Huntington, J.L., Hobbins, M.T., Wood, A., Morton, C., Anderson, M., Hain, C., 2016. The Evaporative Demand Drought Index. Part II: CONUS-Wide Assessment against Common Drought Indicators. J. Hydrometeorol. 17, 1763–1779. https://doi.org/10.1175/JHM-D-15-0122.1

Mckee, T.B., Doesken, N.J., Kleist, J., 1993. The Relationship of Drought Frequency and Duration to Time Scales. Presented at the 8th Conference on Applied Climatology, 17-22 January 1993, Anaheim, pp. 179-184.

Palmer, W.C., 1965. Meteorological drought. Research paper no.45. U.S. Department of Commerce. Weather Bureau, Washington D.C.

Purdy, A.J., Kawata, J., Fisher, J.B., Reynolds, M., Om, G., Ali, Z., Babikian, J., Roman, C., Mann, L., 2019. Designing Drought Indicators. Bull. Am. Meteorol. Soc. 100, 2327–2341. https://doi.org/10.1175/BAMS-D-18-0146.1

Quiring, S.M., 2009. Developing Objective Operational Definitions for Monitoring Drought. J. Appl. Meteorol. Climatol. 48, 1217–1229.

Schmidhuber, J., Tubiello, F.N., 2007. Global food security under climate change. Proc. Natl. Acad. Sci. 104, 19703–19708. https://doi.org/10.1073/pnas.0701976104

Sepulcre-Canto, G., Horion, S., Singleton, A., Carrao, H., Vogt, J., 2012. Development of a Combined Drought Indicator to detect agricultural drought in Europe. Nat. Hazards Earth Syst. Sci. 12, 3519–3531. https://doi.org/10.5194/nhess-12-3519-2012

Slette, I.J., Post, A.K., Awad, M., Even, T., Punzalan, A., Williams, S., Smith, M.D., Knapp, A.K., 2019. How ecologists define drought, and why we should do better. Glob. Change Biol. 25, 3193–3200. https://doi.org/10.1111/gcb.14747

Spinoni, J., Naumann, G., Vogt, J.V., 2017. Pan-European seasonal trends and recent changes of drought frequency and severity. Glob. Planet. Change 148, 113–130. https://doi.org/10.1016/j.gloplacha.2016.11.013

Steinemann, A., Iacobellis, S.F., Cayan, D.R., 2015. Developing and Evaluating Drought Indicators for Decision-Making. J. Hydrometeorol. 16, 1793–1803. https://doi.org/10.1175/JHM-D-14-0234.1

Toonen, W.H.J., Macklin, M.G., Dawkes, G., Durcan, J.A., Leman, M., Nikolayev, Y., Yegorov, A., 2020. A hydromorphic reevaluation of the forgotten river civilizations of Central Asia. Proc. Natl. Acad. Sci. 117, 32982–32988. https://doi.org/10.1073/pnas.2009553117

United States Drought Monitor [WWW Document], 2020. URL https://droughtmonitor.unl.edu/ (accessed 10.23.20).

Vicente-Serrano, S.M., Beguería, S., López-Moreno, J.I., 2010. A Multiscalar Drought Index Sensitive to Global Warming: The Standardized Precipitation Evapotranspiration Index. J. Clim. 23, 1696–1718. https://doi.org/10.1175/2009JCLI2909.1

Wilhite, D.A., Glantz, M.H., 1985. Understanding: the Drought Phenomenon: The Role of Definitions. Water Int. 10, 111–120. https://doi.org/10.1080/02508068508686328

Chapter 1

Evaluation of Drought Stress in Cereal through Probabilistic Modelling of Soil Moisture Dynamics

water

MDPI

Article

Evaluation of Drought Stress in Cereal through Probabilistic Modelling of Soil Moisture Dynamics

María del Pilar Jiménez-Donaire [1,*], Juan Vicente Giráldez [1,2] and Tom Vanwalleghem [1]

[1] Department of Agronomy, University of Córdoba, 14071 Córdoba, Spain; ag1gicej@uco.es (J.V.G.); ag2vavat@uco.es (T.V.)
[2] Institute for Sustainable Agriculture, CSIC, 14071 Córdoba, Spain
* Correspondence: g52jidom@uco.es

Received: 24 August 2020; Accepted: 11 September 2020; Published: 16 September 2020

Abstract: The early and accurate detection of drought episodes is crucial for managing agricultural yield losses and planning adequate policy responses. This study aimed to evaluate the potential of two novel indices, static and dynamic plant water stress, for drought detection and yield prediction. The study was conducted in SW Spain (Córdoba province), covering a 13-year period (2001–2014). The calculation of static and dynamic drought indices was derived from previous ecohydrological work but using a probabilistic simulation of soil moisture content, based on a bucket-type soil water balance, and measured climate data. The results show that both indices satisfactorily detected drought periods occurring in 2005, 2006 and 2012. Both their frequency and length correlated well with annual precipitation, declining exponentially and increasing linearly, respectively. Static and dynamic drought stresses were shown to be highly sensitive to soil depth and annual precipitation, with a complex response, as stress can either increase or decrease as a function of soil depth, depending on the annual precipitation. Finally, the results show that both static and dynamic drought stresses outperform traditional indicators such as the Standardized Precipitation Index (SPI)-3 as predictors of crop yield, and the R^2 values are around 0.70, compared to 0.40 for the latter. The results from this study highlight the potential of these new indicators for agricultural drought monitoring and management (e.g., as early warning systems, insurance schemes or water management tools).

Keywords: drought indicators; drought monitoring; plant water stress; crop yield; Spain

1. Introduction

Drought is one of the main natural hazards affecting agricultural crop production and resulting in food insecurity [1,2]. Kim et al. [3] analyzed the global patterns of crop production losses associated with droughts between 1983 and 2009 and concluded that three-fourths of the global harvested agricultural production areas were affected by drought-induced losses. Leng and Hall [4], analyzing global yield losses for different crops under global change, project that yield loss risk will increase in the future. Moreover, their predictions, using an ensemble of models, show that this risk grows non-linearly with an increase in drought severity. Many drought indices focus on the role of water (e.g., SPI, the standardized precipitation index, including only precipitation), although there is some discussion in the scientific community that heat stress might play an equally or even more important role in this yield decline. In a study on historic crop yields in the US, Ortiz-Bobea et al. [5] found an important effect of water stress, although they point to heat stress as the primary climatic driver of future yield changes under climate change. Especially in water-limited environments, however, studies clearly point to drought as the primary driver [6]. However, it is clear that both drought and extreme heat usually occur simultaneously [7]. Lesk et al. [8] estimate a reduction in cereal production across the globe by 9–10% due to the combined effect of droughts and extreme heat. Climate models project

a particularly worrying increase in the frequency and magnitude of extreme events such as droughts for specific areas such as the Mediterranean. This region is considered to be a drought hotspot. Drought is already of great concern today, and climate projections are especially worrying in the Mediterranean [9]. This is combined with the fact that agriculture plays a vital role in its economy, occupying nearly 50% of its total land area. Rain-fed crops are those most likely to come under pressure first by climate change and droughts, although prolonged droughts will also affect irrigated lands and increase the need for more efficient irrigation systems with higher water-use efficiency [10]. Nearly a fifth (21%) of the Mediterranean region is under irrigation, and agricultural water demand represents over 50% of the total water demand in Mediterranean Europe and 81% in Eastern and Southern Mediterranean countries [11].

In order to respond to and control droughts, by managing food resources, planning policy interventions, or assessing agricultural insurance damage [12], it is crucial to assess their impact on agricultural crop yield in a timely and accurate manner. Over the last decades, researchers have developed various drought indices to understand drought intensity and its effects. Meteorological drought indices—for example, the widely used Standardized Precipitation Index (SPI) [13] or the Standardized Precipitation Evapotranspiration Index (SPEI) [14]—have proven very successful but are limited to easily available climatic data. However, these data are often not available at a high spatial resolution due to the sparse distribution of weather stations. Satellite-based drought indices are widely used in agronomic studies; for example, the Normalized Difference Vegetation Index (NDVI) [15] offers a good proxy for vegetation stress. In recent years, several of these indicators were also used simultaneously in combined drought indicators with good results [16,17]. Peña-Gallardo et al. [18] assessed the performance of different meteorological drought indices in Spain for predicting crop yield and found SPI and SPEI to be best correlated with yield. García Leon et al. [19] analyzed a wider range of drought indices and found that satellite-based indices, in particular, the Vegetation or Temperature Condition Indices (VCI/TCI), were able to explain 70% and 40% of the annual crop yield level and crop yield anomaly variability, respectively, for winter wheat and barley.

A better understanding of how drought impacts agricultural production requires comprehending how drought impacts ecohydrological processes. Ecohydrological research has long focused on the interactions and interrelationships between hydrological processes and the structure and function of vegetation, especially its response to drought. However, not much of this research has made its way into the development of drought indicators, which generally focus on either the description of meteorological patterns alone, through meteorological drought indices (e.g., the SPI, rainfall alone, or the SPEI, the Standardized Precipitation Evapotranspiration Index, using rainfall and potential evapotranspiration), or on the observation of the effects of these droughts on plants (e.g., NDVI-based indices). The modulating effect of soil is not generally taken into account in existing drought indices. However, in ecohydrological literature, such a framework does exist and could be very useful for describing the effects of drought on agricultural crop yield. A modelling framework to describe stochastic soil moisture patterns and their effect on vegetation stress was developed in a series of papers by Laio et al. [20], Porporato et al. [1], and Rodriguez-Iturbe et al. [21]. Their research proposed two important indicators, static and dynamic stresses, to assess the effect of drought on plants and the interaction of soils in this process. However, no direct validation of this methodology was performed.

The objective of this paper is therefore to evaluate the use of static and dynamic stresses as a drought indicator. The specific objectives are to (1) calculate static and dynamic stresses for a test area in SW Spain, (2) assess the sensitivity of these two indicators to rainfall and soil conditions, and, finally, (3) validate their performance as predictors of measured crop yield, in comparison to commonly used drought indicators.

2. Materials and Methods

2.1. Study Area

The study area corresponds to the province of Cordoba, located in the center of Andalusia, SW Spain (Figure 1). This area was selected because yield data were only available at the provincial level (see below). The climate is Mediterranean, with dry, hot summers (Köppen-Geiger climate Csa, [22]). The average annual rainfall for the Cordoba airport station between 1959 and 2018 was 604 mm, with a standard deviation of 243 mm. This high standard deviation illustrates the important interannual variability, with annual rainfall varying between 280 and 1297 mm. The mean annual temperature was 18.0 °C.

Figure 1. Location of study site.

Cereal production in Cordoba province is centered around the Guadalquivir river, and it is part of one of the main cereal-producing areas of Spain [19]. This area is known as the Campiña. The weather station "El Carpio" was selected to be representative for this area (37°54′50″ N, 4°30′14″ W). Soils in the Campiña area are derived from Miocene marls and are typically Vertisols, with a high proportion of expansive clays of ca. 40%. These soils are highly fertile and allow for the typical crop rotation in dryland Mediterranean areas of cereal followed by sunflower during the summer months. Cereal is generally sown during the month of November or early December, depending on the rainfall in that particular year. It is usually harvested during the month of June or early July.

2.2. Calculation of Static and Dynamic Stress Indicators

Porporato et al. [1] propose a model framework to quantify vegetation stress related to the soil moisture conditions, based on key concepts of plant physiology. They define a static, ζ, and a dynamic water stress, θ, the latter also taking into account the temporal dimension in the definition of water stress.

The first drought indicator, static stress, was calculated as a function of stomatal closure. Stomatal closure occurs over the entire scale of water stress and starts with the so-called incipient stomatal closure at a soil moisture content of W^*. The other end of the scale corresponds to complete

stomatal closure, in which the plant starts wilting, corresponding to a soil moisture content called the permanent wilting point, W_{pwp}. Static stress is then defined for the different ranges of soil moisture as

$$\begin{cases} \zeta(t) = 0, \text{ for } W(t) > W^* \\ \zeta(t) = 1, \text{for } W(t) < W_{\mathrm{pwp}} \\ \zeta(t) = \left[\frac{W^* - W(t)}{W^* - W_{\mathrm{pwp}}}\right]^q, \text{ for } W_{\mathrm{pwp}} \leq W(t) \leq W^* \end{cases} \quad (1)$$

These equations show that static stress is taken as being zero when the soil moisture is above the level of incipient stomatal closure, *W**, and that it reaches a maximum value equal to 1 when the soil moisture equals the wilting point. In between these soil moisture values, the vegetation water stress depends on the soil moisture deficit. Plant stress can increase non-linearly with soil moisture deficit, where the coefficient q is a measure of this non-linearity. Porporato et al. [1] suggest that q can vary with plant type and, to a lesser degree, with soil type, although no data exist at present. They suggest a value between 1 and 3, and, in this study, we used a value of 1, implying a linear soil moisture–stress relationship.

The static stress *z(t)* is calculated at a daily time step. The overall static water stress, z, is then calculated by integrating the individual positive values of *z(t)* over time, excluding periods where $z = 0$. This is because the mean value of water stress should indicate those periods in which the plant is actually under stress, and including nil values without stress in the overall mean would lead to an indicator that is not very informative. In this study, we calculated z over the duration of the growing season; for wheat in the study area, this is between November and June, as will be discussed in detail below. This is because, obviously, only plant water stress in this period has an impact on crop yield. When there is no crop present, the soil moisture deficit cannot contribute to the calculated stress index. The same will be valid for dynamic water stress.

The development of the second indicator, dynamic stress, stems from the realization that the linkage of soil moisture dynamics and plant water stress is a complex problem, due to the stochastic nature of the soil moisture dynamics and the complexity of plant responses [1]. Static stress only takes into account the mean intensity of the plant water deficit but contains no information on its duration and frequency. Therefore a second indicator is proposed, a dynamic stress index that couples the static stress, which represents the integrated effect of the excursion of soil moisture below a critical level *W**, with the mean duration and frequency of these stress events, termed, respectively, T_{W^*} and n_{W^*}, as follows:

$$\begin{cases} \theta = \left(\frac{\zeta\, T_{W*}}{k\, T_{seas}}\right)^{1/\sqrt{n_{W*}}}, \text{ if } \zeta\, T_{W*} < k\, T_{seas} \\ \theta = 1\,, \textit{ otherwise} \end{cases} \quad (2)$$

where T_{seas} is the duration of the growing season and k is a parameter.

The rationale behind this equation is explained in detail by Porporato et al. [1]. Briefly, the idea behind it is that the same value of z can have a very different effect depending on whether drought occurs as frequent, small episodes or as one, longer episode. For simplicity, it is assumed that a linear relation exists between vegetation stress and the duration of that stress. At present, no data exist to justify a non-linear relation. Therefore, q relates directly to the product of zT_{W^*}. However, the actual vegetation stress cannot increase indefinitely with zT_{W^*}. The upper value is fixed by the parameter k, so permanent plant damage occurs when $zT_{W^*} > kT_{seas}$, and in these cases, the value of q reaches its maximum of 1. The value of k is set to 0.5, following Porporato et al. [1].

2.3. Soil Water Balance

To calculate the soil water balance, we followed the same approach presented by Jiménez-Donaire et al. [17]. Soil moisture dynamics are calculated with a simple bucket model, using a volume-balance equation applied over the root zone and taking into account the main processes

of infiltration, evapotranspiration and deep seepage. Therefore, the calculated soil moisture values are representative of the average moisture content over the root-zone depth, h.

To evaluate the soil moisture dynamics, the simple water balance model of [23] was used. In this model, the water depth in the soil profile, W, evolves with time, t, following the contribution of the infiltration of the rain, f, and the extraction of the evapotranspiration, e, and of the deep percolation or of the surface and subsurface runoff, g. The balance was computed at the daily time scale:

$$\frac{dW(t)}{dt} = f - e - g \tag{3}$$

The infiltration depth is estimated from the rain depth, p; the wetness or relative soil water content, normalized by the maximum value, $Wmax$, so $\omega = W/Wmax$; and a parameter m, with the empirical approximation proposed by Georgakakos [24]:

$$f = p(1 - \omega^m) \tag{4}$$

The deep percolation or runoff loss is estimated by a simple potential function with the saturated hydraulic conductivity, k_s, and λ, the index of pore size distribution of Brooks and Corey [25].

$$g = k_s \omega^{3+2/\lambda} \tag{5}$$

Finally, the daily evapotranspiration rate is estimated as the FAO Penman–Monteith [26] potential rate, e_0, modified by the wetness and the crop coefficient, k_c:

$$e = \omega k_c e_0 \tag{6}$$

The values for k_c for cereal were set at 0.35 (November to December), 0.75 (January to February), 1.15 (March to May) and 0.45 (June), following recommendations by FAO [27]. The other relevant variables used in the water balance are cited in Table 1.

Table 1. Main soil and plant parameters used in the soil water balance and to calculate plant stress.

Parameter	Value	Source
m (-)	0.1	Mean value of the interval proposed by Brocca et al. [23]
Ks (mm day^{-1})	38.4	Estimate of soil water properties by Rawls and Brakensiek [28]; representative value for clay soil according to USDA classification
λ (-)	0.15	Derived from graphics of the parameter l of Brooks and Corey [25] as a function of soil texture, organic matter content and increase in soil porosity above the reference [29]
Ws (m^3/m^3)	0.45	As proposed by Vanderlinden [30] calculated from the soil map of Andalusia
W_{fc} (m^3/m^3)	0.32	
W_{pwp} (m^3/m^3)	0.22	
W_r (m^3/m^3)	0.05	
W^* (m^3/m^3)	0.275	Following Doorenbos en Pruitt [27], taken as 55% of the total available water for cereal
q (-)	1	Porporato et al. [1]
k (-)	0.5	Porporato et al. [1]
h (m)	1	Fan et al. [31]

2.4. Crop Yield Data

Harvest data spanning the years 2003 to 2015 were collected from the Ministry of Agriculture, Fisheries and Food [32], with these statistics being pooled at the provincial level. For this study, focusing on wheat crop yields, we used the data for the Cordoba province, as this is an area representative of one of the main cereal-growing areas in Mediterranean Spain, as mentioned above. The total wheat production area changed over time, from 146,837 ha in 2003 to 84,314 ha in 2015, of which 77–90% is rainfed. The irrigated wheat crop area occupies about 14,000 ha and has remained more constant over this period. It was not taken into account for this study, as it is not likely to be affected equally by drought.

3. Results

3.1. Soil Moisture Dynamics

Rainfall is very seasonal in the study area, with a clearly defined wet and dry season. It is also highly variable within the study period, with values ranging between 274.8 mm (year 2012) and 853.4 mm (year 2010). This rainfall forcing creates a clearly bimodal probability distribution function of soil moisture, with two marked peaks, shown in Figure 2. The results shown here represents normalized soil moisture values, i.e., $S = (W - W_r)/(W_s - W_r)$, over the entire study period, from 2001–2014. Values of 0 correspond to a soil moisture status equal to residual soil moisture, while values of 1 represent total soil saturation. This figure clearly shows how this bimodal distribution is the resulting sum of a well-marked dry and wet season (respectively, represented in brown, taken from May to October, and blue, taken from November to April). The lower peak, corresponding to the dry season, is close to 0.18, and the other peak, corresponding to the wet season, is around 0.65. The mean overall relative soil moisture is 0.37, with minimum values close to 0 and a maximum value of 0.78. These results provide a good indication that the established water balance model performs well. This is typical for Mediterranean areas, and, although there are no soil moisture measurements available for the study site under cereal, in situ soil moisture observations at a nearby site under olive cultivation showed a very similar bimodal probability density function [33]. These authors also observed a dominating peak corresponding to dry soils for residual water content and another, lower peak at intermediate soil moisture values. To show the variation in soil moisture over the year better, Figure 3 depicts the evolution of normalized soil moisture, S, over the year. In this figure, the mean value of soil moisture is shown in bold, and the gray areas represent the 5 to 95% percentiles, calculated based on daily values of the 2001–2014 period. This figure clearly shows that during the summer dry period, soil moisture drops to a minimum and its variability is about half of that in the wet winter period. This means that all the years analyzed are characterized by an absence of rainfall in this period and a drying out of the soil to values a little above residual soil water content. Around October, the soil moisture starts rising again sharply as the soils are replenished by rainfall. In this period, the variability also rises sharply, as during some wet years, the soil water content is close to its maximum by October, and in other years, the soil moisture remains dry throughout the fall and winter. This can especially be seen in the 5th percentile lower values remaining low. After January, the average soil moisture remains constant until March, after which it drops steadily, although, during wet years, soil moisture can remain high till May, while in dry years, as mentioned before, the soil is never replenished.

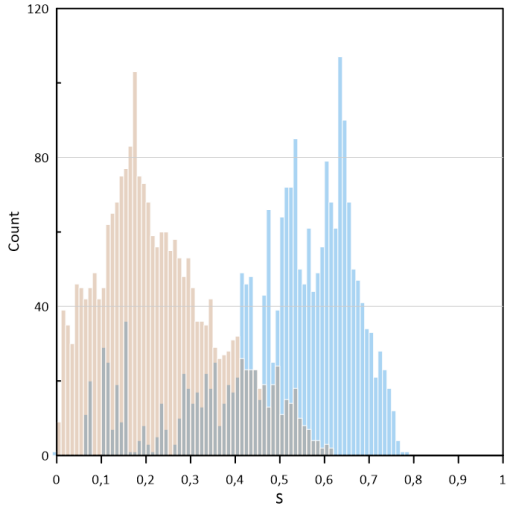

Figure 2. Probability distribution of modelled normalized soil moisture, separated into dry and wet seasons (brown and blue, respectively).

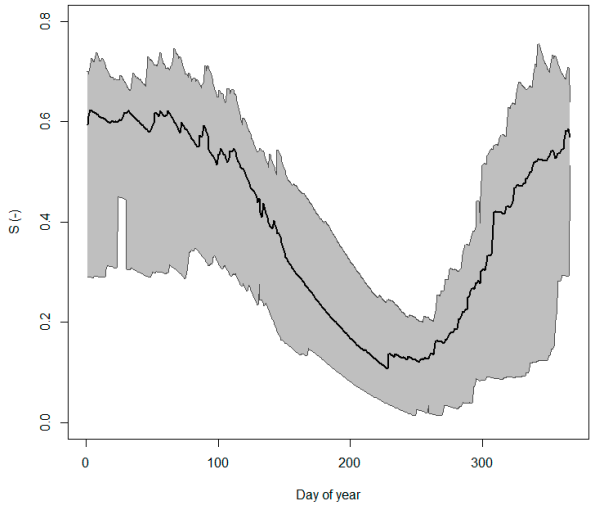

Figure 3. Evolution of the seasonal variation of normalized soil moisture, *S*, over the year. Thick line indicates mean values, and gray zone indicates 5 to 95% quantiles.

3.2. Static and Dynamic Stress Indicators

Figure 4 shows the evolution of the modelled soil moisture over the study period, in blue, and the resulting static plant water stress, in gray. The extension of each growing season is indicated in green. Static stress generally drops to 0 during the wet winter months and rises to a maximum value of 1 as soon as the soil dries out in spring. Due to the dry Mediterranean summer, it is normal to have a maximum static stress value of 1 outside of the growing season, but these values were not taken into account for the overall yearly calculation. The dry period between 2005 and 2006 is interesting, as these were particularly dry years, and the soil moisture during these years remained low. Therefore, the resulting static stress values remained at a maximum throughout the 2006 growing season. The same happened in 2012. On the other hand, the 2008 growing season was one of the years with the lowest static stress values.

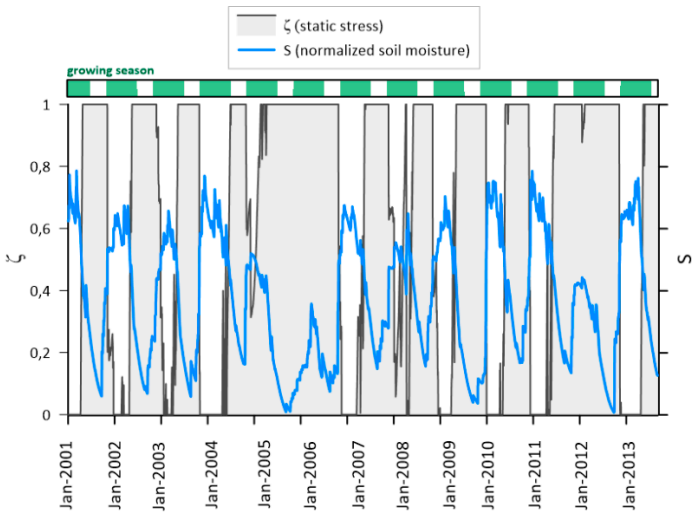

Figure 4. Evolution of normalized soil moisture (blue) and static stress (gray) over the study period. Growing season extent is indicated in green.

The dynamic stress is calculated based on the static stress but also taking into account the number and mean duration of the stress events throughout the growing season, as described earlier. This indicator is therefore only calculated once for each growing season. Figure 5 shows how both variables, the number and mean duration of the drought stress events (n_{W^*} and T_{W^*}, respectively),

are related to annual precipitation. This figure clearly shows how the dry years are characterized by a single, long stress event. Three years are characterized by a single stress period ($n_{W^*} = 1$) that lasts almost the entire growing season (8 months or 243 days). These years correspond to the growing seasons of 2005, 2006 and 2012 (the hydrological years of 2004–2005, 2005–2006 and 2011–2012, respectively), with an annual precipitation of around 300 mm, i.e., less than half the average annual precipitation in this area. Wetter years are characterized by more frequent, but shorter, stress periods. The number of stress periods increased linearly with annual precipitation, while their duration decreased exponentially. In both cases, the fit was significant, although the scatter was high, resulting in a moderate fit with R^2 values of 0.40 and 0.50, respectively. The relationship between the number of stress periods and annual precipitation is probably not linear but, rather, characterized by a maximum value and then drops to 0 for higher values of annual precipitation. However, in the study area, this did not occur during the analyzed time period.

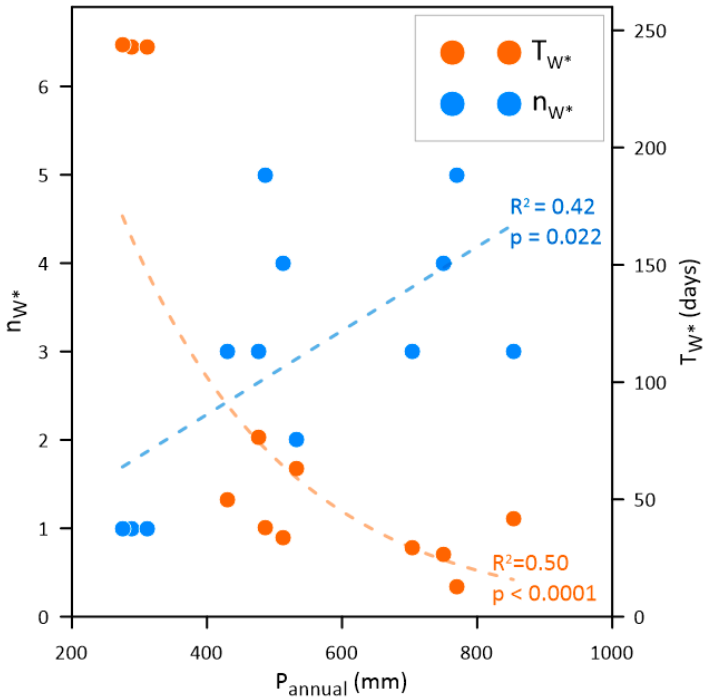

Figure 5. Relation of number (n_{W^*}) and mean duration (T_{W^*}) of drought stress events with annual precipitation (P_{anual}).

Finally, the relation between the static and the dynamic stress is shown in Figure 6 and is fitted by a power relationship. Although this is not the best possible fit in existence, it is used for theoretical considerations, as a power relationship can be deduced from Equation (2). In this equation, a power relation can be derived between static and dynamic stresses if the other variables do not vary too much. Indeed, it can be seen that the values of the product kT_{seas} remain constant for a given crop type, in this case, cereal. The variation in the other two variables, the number and length of drought stress events, n_{W^*} and T_{W^*}, is shown in Figure 5. T_{W^*} is generally around 50 days, as most years have multiple short drought periods, except for three years with a single drought that lasts the whole growing season (8 months or 243 days). This power relationship is of interest for characterizing the soil–climate–plant system.

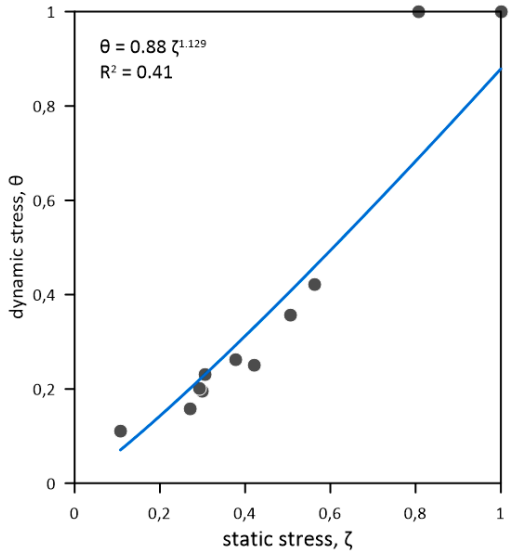

Figure 6. Dynamic versus static stress.

3.3. Sensitivity of Static and Dynamic Stress Indicators to Soil Depth

As discussed previously, the two stress indicators are closely related to the amount and distribution of the rainfall during the growing season. However, another important variable is the soil type; the soil acts as a reservoir to store water and supply it to the plant when needed. The calculation of soil stress is therefore closely related to the water buffering capacity of the soil, expressed by its total available soil water content. This variable is calculated from the soil depth and from soil water retention behavior, which varies as a function of soil texture and structure. The sensitivity of static and dynamic stresses to the soil water buffering capacity is analyzed here by varying the soil depth. It is assumed here that plant roots can explore the full soil depth, and therefore, soil depth is the limiting variable for root-zone soil moisture storage. This variable is used here to change the soil water-holding capacity, so the same result could be obtained by varying the soil texture or structure, although these variables are not analyzed explicitly. Soil depth can be used as a proxy for both, as, for example, the effect of increasing the pore space would be the same as that of increasing the soil depth. Figure 7 shows the variation of static and dynamic stresses in relation to soil depth. A complex behavior emerges that can be better understood as a function of annual precipitation. Therefore, the different years that fall within the study period were classified into four groups from lower to higher total annual precipitation (brown to blue color). Static and dynamic stresses behave similarly, with small differences that will be analyzed in detail. First of all, for low precipitation values (<431 mm), static and dynamic stresses both increase with soil depth. This increase is gradual for static stress and quite abrupt for dynamic stress. For higher precipitation values (>513 mm), static and dynamic stresses decrease with soil depth. A third group of precipitation values fall in between both behaviors, and first decrease (up to 600 mm soil depth) and then increase.

The reason for the increase with soil depth for lower precipitation values (below 431 mm) is that if both are low, the stress in the system increases for larger soil depths, as the same amount of rainfall results in a lower soil moisture content since the water infiltrates deeper and is averaged out over a larger soil volume. Since the rainfall is so low, there is no benefit from the existence of deep, fertile soils under these conditions. Sites with this soil–rainfall combination would be highly unsuitable for cereal growth. As soon as the rainfall increases, especially for the two classes above 513 mm, it can be seen that deeper soils actually benefit plant growth and reduce plant water stress. The excess soil moisture can be stored under these circumstances, and during dry periods, as long as they are not too pronounced, the soil system can keep up with plant water uptake. The third group (413–513 mm) falls in between both behaviors.

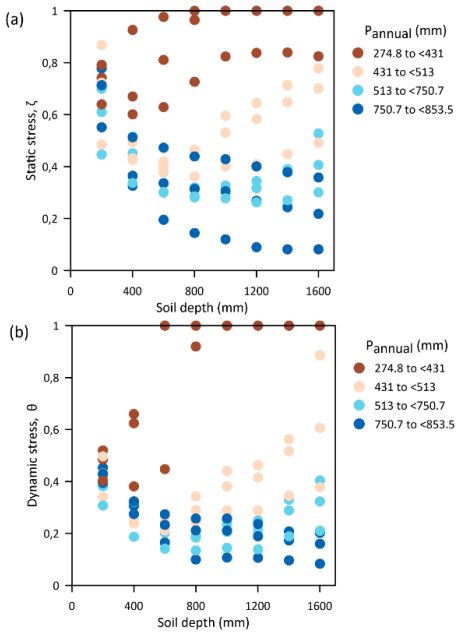

Figure 7. Sensitivity of the (**a**) static and (**b**) dynamic stress to soil depth. Color codes show the annual precipitation classified into four levels.

3.4. Validation of Static and Dynamic Stresses for Prediction of Crop Yield

It has become clear from previous results that both plant water stress indicators are straightforward to calculate, and the complex response to annual precipitation and soil characteristics has been assessed. The key question that remains is whether these new stress-based drought indicators are of practical use for the prediction of crop yield.

Figure 8 shows the prediction of crop yield as a function of three different drought indicators: the two drought indicators that were evaluated in this study, static and dynamic stresses, and a commonly used drought indicator, SPI-3. Both static and dynamic stresses are shown to be very good indicators, with R^2 values of 0.77 and 0.78, respectively. By comparison, SPI-3 performs very poorly. This is surprising given that other studies generally report a reasonable performance of this indicator. It should be noted that one year, marked in red, was considered an outlier. The reason for this is that this point corresponds to the 2006 growing season. During that year, significantly less surface area of rainfed wheat was sown by farmers (−30%), as a response to the bad harvests in the wake of the 2005 drought. This probably resulted in an artificially high average crop yield for that year, compared to other years, as more marginal lands were taken out of production.

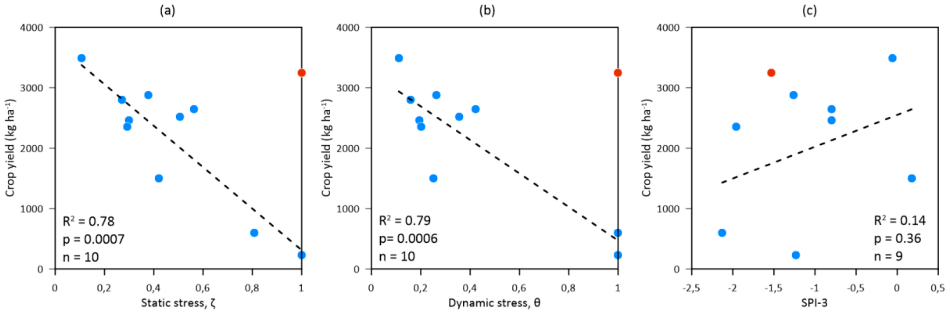

Figure 8. Prediction of crop yield as a function of different drought indicators: (**a**) static stress, (**b**) dynamic stress and (**c**) Standardized Precipitation Index (SPI)-3. Note that the red dots indicate outliers that were not taken into account; see text for details.

4. Discussion

The results of the sensitivity analysis show a high response of the static and dynamic stresses to soil depth. This shows how important it is to take into account soil properties and plant rooting depth in drought prediction and how both variables can modulate the effect of meteorological conditions on plant water stress. Different soil-moisture-based drought indicators are being developed and tested, although accurate information on soil depth or properties is often missing in these models. Sepulcre-Canto et al. [16] use a Soil Moisture Anomaly index as part of their combined drought indicator. This index is calculated using the LISFLOOD model at a very coarse resolution of 5 km. While useful for continental-scale predictions, the model's simplifications and spatial scale may make it result in a large approximation of the actual soil moisture content and render it less accurate on the farm scale or for agricultural crop yield predictions. A similar multi-indicator approach was tested by Jiménez-Donaire et al. [17], who included a soil moisture deviation as one of the three indicators that made up the drought index and concluded that it corresponded well to agricultural insurance claim data. Narasimhan and Srinivasan [34] developed the Soil Moisture Deficit Index (SMDI), which draws on the hydrological model SWAT, but, again, the spatial resolution is rather coarse (16 km^2). Sohrabi et al. [35] developed a specific soil moisture drought index, named SODI, to characterize droughts by calculating the deviation of soil moisture from field capacity. When it was tested in Idaho (USA), the authors concluded that this index outperformed other drought indices such as the standardized precipitation index (SPI), the standardized precipitation evapotranspiration index (SPEI) and the Palmer drought index. However, this is based only on an intercomparison between these drought indices, as they do not use external datasets such as agricultural crop yield data to validate these results. Other promising approaches have relied on the remote sensing of soil moisture rather than modelling in situ soil moisture. For example, Martínez-Fernández et al. [36] developed the Soil Water Deficit Index (SWDI), and Sánchez et al. [37], the Soil Moisture Agricultural Drought Index (SMADI), based on SMOS and MODIS/SMOS products. The remote sensing of soil moisture has the disadvantage that it is only sensitive to superficial moisture [38]; for example, a SMAP radiometer can measure soil moisture up to a 5 cm depth under optimal conditions [39]. However, different studies have shown a good correlation of in situ root-zone soil moisture measurements with remotely sensed superficial soil moisture data [39] or with specifically developed root-zone soil moisture products, such as the 0–100 cm L4_SM that combines the advantages of spaceborne L-band brightness temperature measurements, precipitation observations and land surface modeling with [38,40]. This type of work shows that there is good potential for satellite-based soil moisture drought indices, although, as far as the authors are aware, validation against independent crop yield data, as was performed in this study, has not yet been performed.

Finally, this study also shows the importance of rooting depth for assessing crop sensitivity to drought. This implies that when assessing the agricultural effects of droughts, it is crucial to make specific calculations for different crops. In presently used indicators, this is generally not included, as many drought indicators use reference crop evapotranspiration, and those that take into account soil moisture, a single value for soil properties. This shows that future research should be geared towards combining land use maps with drought indicators to develop specific evaluations for different crop types. In short, our results show that it is of critical importance to correctly estimate root-zone soil moisture in order to calculate drought indices, as both soil depth and rooting depth influence this variable. Our study has performed this through probabilistic modelling because of the long time frame involved, but other approaches using remote sensing products and data assimilation for the estimation of root-zone soil moisture are promising [39,41].

With regard to crop type, it is also important to consider the stage of crop growth. In this study, water stress is currently considered to be equally important throughout the growing season. However, we know that there are certain stages of plant development that are more susceptible than others. Further research could focus on taking this into account, for example, by giving larger weight to drought stress in these periods in the calculation of the overall indicator. However, this escapes the

objectives of this study, whose aim was to test these two simple stress indicators, in the form in which they were designed by Porporato et al. [1]. Further research should aim at perfecting these to obtain even better crop yield predictions.

5. Conclusions

This study evaluated two novel indices for drought prediction, static and dynamic plant water stress. These indices are based on early work in ecohydrology by Porporato et al. [1]. Both indices are calculated from simulated soil moisture and take into account the stress that a soil moisture deficit induces on plants. The simulation of soil moisture yields good results, with a bimodal probability distribution that can be clearly divided into two separate populations, one corresponding to the dry season and the other, to the wet season. These results are similar to those of field studies using soil moisture sensors that reported a similar bimodal probability distribution function.

Static and dynamic stresses were shown to detect and correctly quantify the occurrence of dry years in the study period. The number and length of drought periods, two variables taken into account to calculate dynamic stress, were shown to decrease and increase, respectively, with increasing annual precipitation. Both static and dynamic stresses were shown to be highly sensitive to soil depth, and their response behavior, increasing or decreasing, was found to be dependent on total annual precipitation.

Finally, the most important result of this study is that both indicators were found to be good predictors of crop yield. The advantage of these two new indicators, compared to meteorological indices, such as SPI or SPEI, is that the buffering effect of the soil's water holding capacity is taken into account. Therefore, the static and dynamic stresses were found to be superior to the SPI in terms of crop yield prediction, at least in the water-limited conditions of Southern Spain.

In conclusion, both static and dynamic water stress are useful indices for drought detection and quantification. Both indices are easily computed using limited datasets. Where more detailed data are available, these indices can account for the type and depth of soil, in order to calculate spatially distributed drought indices. In addition, they allow one to consider the effect of the length of the growing season and the type of crop by selecting different threshold soil moisture levels for the onset of plant water stress. While this study focused on cereal, further research could focus on evaluating the potential of these indices in other crops or on determining these threshold values for different crops.

Author Contributions: Conceptualization, J.V.G. and T.V.; methodology, M.d.P.J.-D.; software, M.d.P.J.-D. and T.V.; formal analysis, M.d.P.J.-D.; investigation, M.d.P.J.-D. and T.V.; writing—original draft preparation, M.d.P.J.-D.; writing—review and editing, M.d.P.J.-D., J.V.G. and T.V.; visualization, M.d.P.J.-D. and T.V.; supervision, J.V.G. and T.V.; project administration, T.V.; funding acquisition, T.V. All authors have read and agreed to the published version of the manuscript.

Funding: This study was funded by the research project PID2019-109924RB-I00 financed by the "Programas estatales de generación de conocimiento y fortalecimiento científico y tecnológico del sistema de I+D+i y de I+D+i orientada a los retos de la sociedad".

Acknowledgments: The climate data were obtained from the Agroclimatic network of Andalusia ("Red de Información Agroclimática de Andalucía") and were kindly provided by the Instituto de Investigación y Formación Agraria y Pesquera of the Consejería de Agricultura, Ganadería, Pesca y Desarrollo of the Junta de Andalucía.

Conflicts of Interest: The authors declare no conflict of interest.

References

1. Porporato, A.; Laio, F.; Ridolfi, L.; Rodriguez-Iturbe, I. Plants in water-controlled ecosystems: Active role in hydrologic processes and response to water stress: III. Vegetation water stress. *Adv. Water Resour.* **2001**, *24*, 725–744. [CrossRef]
2. Enenkel, M.; See, L.; Bonifacio, R.; Boken, V.; Chaney, N.; Vinck, P.; You, L.; Dutra, E.; Anderson, M. Drought and food security—Improving decision-support via new technologies and innovative collaboration. *Glob. Food Secur.* **2015**, *4*, 51–55. [CrossRef]

3. Kim, W.; Iizumi, T.; Nishimori, M. Global Patterns of Crop Production Losses Associated with Droughts from 1983 to 2009. *J. Appl. Meteorol. Climatol.* **2019**, *58*, 1233–1244. [CrossRef]
4. Leng, G.; Hall, J. Crop yield sensitivity of global major agricultural countries to droughts and the projected changes in the future. *Sci. Total Environ.* **2019**, *654*, 811–821. [CrossRef]
5. Ortiz-Bobea, A.; Wang, H.; Carrillo, C.M.; Ault, T.R. Unpacking the climatic drivers of US agricultural yields. *Environ. Res. Lett.* **2019**, *14*, 064003. [CrossRef]
6. Dai, A. Drought under global warming: A review. *WIREs Clim. Chang.* **2011**, *2*, 45–65. [CrossRef]
7. Hussain, H.A.; Men, S.; Hussain, S.; Chen, Y.; Ali, S.; Zhang, S.; Zhang, K.; Li, Y.; Xu, Q.; Liao, C.; et al. Interactive effects of drought and heat stresses on morpho-physiological attributes, yield, nutrient uptake and oxidative status in maize hybrids. *Sci. Rep.* **2019**, *9*, 3890. [CrossRef] [PubMed]
8. Lesk, C.; Rowhani, P.; Ramankutty, N. Influence of extreme weather disasters on global crop production. *Nature* **2016**, *529*, 84–87. [CrossRef]
9. Spinoni, J.; Barbosa, P.; Bucchignani, E.; Cassano, J.; Cavazos, T.; Christensen, J.H.; Christensen, O.B.; Coppola, E.; Evans, J.; Geyer, B.; et al. Future Global Meteorological Drought Hot Spots: A Study Based on CORDEX Data. *J. Clim.* **2020**, *33*, 3635–3661. [CrossRef]
10. Rey, D.; Holman, I.P.; Knox, J.W. Developing drought resilience in irrigated agriculture in the face of increasing water scarcity. *Reg. Environ. Chang.* **2017**, *17*, 1527–1540. [CrossRef]
11. Daccache, A.; Ciurana, J.S.; Diaz, J.A.R.; Knox, J.W. Water and energy footprint of irrigated agriculture in the Mediterranean region. *Environ. Res. Lett.* **2014**, *9*, 124014. [CrossRef]
12. Mann, M.L.; Warner, J.M.; Malik, A.S. Predicting high-magnitude, low-frequency crop losses using machine learning: An application to cereal crops in Ethiopia. *Clim. Chang.* **2019**, *154*, 211–227. [CrossRef]
13. Mckee, T.B.; Doesken, N.J.; Kleist, J. The Relationship of Drought Frequency and Duration to Time Scales. In Proceedings of the Eighth Conference on Applied Climatology, Anaheim, CA, USA, 17–22 January 1993; pp. 179–184.
14. Vicente-Serrano, S.M.; Beguería, S.; López-Moreno, J.I. A Multiscalar Drought Index Sensitive to Global Warming: The Standardized Precipitation Evapotranspiration Index. *J. Clim.* **2010**, *23*, 1696–1718. [CrossRef]
15. Gao, X.-D.; Katsumoto, T.; Onodera, K. Purification and Characterization of Chitin Deacetylase from Absidia coerulea. *J. Biochem.* **1995**, *117*, 257–263. [CrossRef]
16. Sepulcre-Canto, G.; Horion, S.; Singleton, A.; Carrao, H.; Vogt, J. Development of a Combined Drought Indicator to detect agricultural drought in Europe. *Nat. Hazards Earth Syst. Sci.* **2012**, *12*, 3519–3531. [CrossRef]
17. Jiménez-Donaire, M.D.P.; Tarquis, A.; Giráldez, J.V. Evaluation of a combined drought indicator and its potential for agricultural drought prediction in southern Spain. *Nat. Hazards Earth Syst. Sci.* **2020**, *20*, 21–33. [CrossRef]
18. Peña-Gallardo, M.; Vicente-Serrano, S.M.; Domínguez-Castro, F.; Beguería, S. The impact of drought on the productivity of two rainfed crops in Spain. *Nat. Hazards Earth Syst. Sci.* **2019**, *19*, 1215–1234. [CrossRef]
19. García-León, D.; Contreras, S.; Hunink, J. Comparison of meteorological and satellite-based drought indices as yield predictors of Spanish cereals. *Agric. Water Manag.* **2019**, *213*, 388–396. [CrossRef]
20. Laio, F.; Porporato, A.; Ridolfi, L.; Rodriguez-Iturbe, I. Plants in water-controlled ecosystems: Active role in hydrologic processes and response to water stress: II. Probabilistic soil moisture dynamics. *Adv. Water Resour.* **2001**, *24*, 707–723. [CrossRef]
21. Rodriguez-Iturbe, I.; Porporato, A.; Laio, F.; Ridolfi, L. Plants in water-controlled ecosystems: Active role in hydrologic processes and response to water stress: I. Scope and general outline. *Adv. Water Resour.* **2001**, *24*, 695–705. [CrossRef]
22. Peel, M.C.; Finlayson, B.L.; McMahon, T.A. Updated world map of the Köppen-Geiger climate classification. *Hydrol. Earth Syst. Sci.* **2007**, *11*, 1633–1644. [CrossRef]
23. Brocca, L.; Melone, F.; Moramarco, T. On the estimation of antecedent wetness conditions in rainfall–runoff modelling. *Hydrol. Process.* **2008**, *22*, 629–642. [CrossRef]
24. Georgakakos, K.P. A generalized stochastic hydrometeorological model for flood and flash-flood forecasting: 1. Formulation. *Water Resour. Res.* **1986**, *22*, 2083–2095. [CrossRef]
25. Brooks, R.H.; Corey, A.T. Properties of Porous Media Affecting Fluid Flow. *J. Irrig. Drain. Div.* **1966**, *92*, 61–88.

26. Allen, R.G.; Pereira, L.S.; Raes, D.; Smith, M. *Crop Evapotranspiration: Guidelines for Computing Crop Water Requirements*; FAO Irrigation and Drainage Paper; Food and Agriculture Organization of the United Nations: Rome, Italy, 1998; ISBN 978-92-5-104219-9.
27. Doorenbos, J.; Pruitt, W.O. *Guidelines for Predicting Crop Water Requirements*; FAO Irrigation and Drainage Paper 24; Rev; Food and Agriculture Organization of the United Nations: Rome, Italy, 1977; ISBN 978-92-5-100279-7.
28. Rawls, W.J.; Brakensiek, D.L. Estimation of Soil Water Retention and Hydraulic Properties. In *Unsaturated Flow in Hydrologic Modeling: Theory and Practice*; NATO ASI Series; Morel-Seytoux, H.J., Ed.; Springer: Dordrecht, The Netherlands, 1989; pp. 275–300, ISBN 978-94-009-2352-2.
29. Rawls, W.J.; Brakensiek, D.L.; Soni, B. Agricultural Management Effects on Soil Water Processes Part I: Soil Water Retention and Green and Ampt Infiltration Parameters. *Trans. ASAE* **1983**, *26*, 1747–1752. [CrossRef]
30. Vanderlinden, K. *Análisis de Procesos Hidrológicos a Diferentes Escalas Espacio-Temporales*; University of Córdoba, Dept. of Agronomy: Córdoba, Spain, 2001.
31. Fan, J.; McConkey, B.; Wang, H.; Janzen, H. Root distribution by depth for temperate agricultural crops. *Field Crop. Res.* **2016**, *189*, 68–74. [CrossRef]
32. Ministerio de Agricultura, Pesca y Alimentación Anuario de Estadística. Available online: https://www.mapa.gob.es/es/estadistica/temas/publicaciones/anuario-de-estadistica/ (accessed on 15 August 2020).
33. Espejo-Pérez, A.J.; Brocca, L.; Moramarco, T.; Giráldez, J.V.; Triantafilis, J.; Vanderlinden, K. Analysis of soil moisture dynamics beneath olive trees. *Hydrol. Process.* **2016**, *30*, 4339–4352. [CrossRef]
34. Narasimhan, B.; Srinivasan, R. Development and evaluation of Soil Moisture Deficit Index (SMDI) and Evapotranspiration Deficit Index (ETDI) for agricultural drought monitoring. *Agric. For. Meteorol.* **2005**, *133*, 69–88. [CrossRef]
35. Sohrabi, M.M.; Ryu, J.H.; Abatzoglou, J.; Tracy, J. Development of Soil Moisture Drought Index to Characterize Droughts. *J. Hydrol. Eng.* **2015**, *20*, 04015025. [CrossRef]
36. Martínez-Fernández, J.; González-Zamora, A.; Sánchez, N.; Gumuzzio, A.; Herrero-Jiménez, C.M. Satellite soil moisture for agricultural drought monitoring: Assessment of the SMOS derived Soil Water Deficit Index. *Remote Sens. Environ.* **2016**, *177*, 277–286. [CrossRef]
37. Sánchez, N.; González-Zamora, Á.; Piles, M.; Martínez-Fernández, J. A New Soil Moisture Agricultural Drought Index (SMADI) Integrating MODIS and SMOS Products: A Case of Study over the Iberian Peninsula. *Remote Sens.* **2016**, *8*, 287. [CrossRef]
38. Reichle, R.H.; De Lannoy, G.J.M.; Liu, Q.; Ardizzone, J.V.; Colliander, A.; Conaty, A.; Crow, W.; Jackson, T.J.; Jones, L.A.; Kimball, J.S.; et al. Assessment of the SMAP Level-4 Surface and Root-Zone Soil Moisture Product Using In Situ Measurements. *J. Hydrometeorol.* **2017**, *18*, 2621–2645. [CrossRef]
39. Velpuri, N.M.; Senay, G.B.; Morisette, J.T. Evaluating New SMAP Soil Moisture for Drought Monitoring in the Rangelands of the US High Plains. *Rangelands* **2016**, *38*, 183–190. [CrossRef]
40. Zhuang, R.; Zeng, Y.; Manfreda, S.; Su, Z. Quantifying Long-Term Land Surface and Root Zone Soil Moisture over Tibetan Plateau. *Remote Sens.* **2020**, *12*, 509. [CrossRef]
41. Baldwin, D.; Manfreda, S.; Keller, K.; Smithwick, E.A.H. Predicting root zone soil moisture with soil properties and satellite near-surface moisture data across the conterminous United States. *J. Hydrol.* **2017**, *546*, 393–404. [CrossRef]

Chapter 2

Evaluation of a combined drought indicator and its potential for agricultural drought prediction in Southern Spain

Nat. Hazards Earth Syst. Sci., 20, 21–33, 2020
https://doi.org/10.5194/nhess-20-21-2020

Natural Hazards and Earth System Sciences
Open Access
EGU

Evaluation of a combined drought indicator and its potential for agricultural drought prediction in southern Spain

María del Pilar Jiménez-Donaire[1], **Ana Tarquis**[2,3], **and Juan Vicente Giráldez**[1,4]

[1]Department of Agronomy, University of Córdoba, Córdoba, 14071, Spain
[2]CEIGRAM, Universidad Politécnica de Madrid, Madrid, 28040, Spain
[3]Grupo de Sistemas Complejos, Universidad Politécnica de Madrid, Madrid, 28040, Spain
[4]Institute for Sustainable Agriculture, CSIC, Cordova, 14071, Spain

Correspondence: María del Pilar Jiménez-Donaire (p.jimenez.donaire@gmail.com)

Received: 19 April 2019 – Discussion started: 29 April 2019
Revised: 26 September 2019 – Accepted: 30 October 2019 – Published: 3 January 2020

Abstract. Drought prediction is crucial, especially where the rainfall regime is irregular, such as in Mediterranean countries. A new combined drought indicator (CDI) integrating rainfall, soil moisture and vegetation dynamics is proposed. Standardized precipitation index (SPI) is used for evaluating rainfall trends. A bucket-type soil moisture model is employed for keeping track of soil moisture and calculating anomalies, and, finally, satellite-based normalized difference vegetation index (NDVI) data are used for monitoring vegetation response. The proposed CDI has four levels, at increasing degrees of severity: watch, warning, alert type I and alert type II.

This CDI was thus applied over the period 2003–2013 to five study sites, representative of the main grain-growing areas of SW Spain. The performance of the CDI levels was assessed by comparison with observed crop damage data.

Observations show a good match between crop damage and the CDI. Important crop drought events in 2004–2005 and 2011–2012, distinguished by crop damage in between 70 % and 95 % of the total insured area, were correctly predicted by the proposed CDI in all five areas.

1 Introduction

Drought is a recurrent phenomenon on the Earth's surface. It is triggered by lack of water, or "an extended imbalance between supply and demand" in the precise expression of Hobbins et al. (2016), and may have economic, social and environmental impacts (Wilhite, 2000). Drought is one of the most important natural disasters threatening our society. In spite of its relevance, there is no proper definition of drought. Tannehill (1947) called drought "the creeping phenomenon", given the complexity of accurately delimiting its start time and end time and of adequately demarcating the spatial extent of its effects.

Wilhite and Glantz (1985) distinguished four main types of droughts according to how the effects were noticed: (i) meteorological, due to the scarcity of rainfall; (ii) hydrological, detected by low streamflow; (iii) agricultural, when soil water is not sufficient to maintain a crop; and (iv) socioeconomic, when it affects the normal functioning of society.

Drought occurs worldwide but it is especially frequent in the Mediterranean region. In a recent analysis of a tree-ring-based reconstruction of the summer season, the Palmer drought severity index (PDSI) (Keyantash and Dracup, 2002) for the period from 1100 to 2012, Cook et al. (2015, 2016) detected the gravity of recent events in the area, which were apparently induced by anthropogenic activity. Combining two drought indices, one meteorological, the Standardized Precipitation Index (SPI), for water supply, and the other hydrological, the standardized precipitation–evapotranspiration index (SPEI), for water loss tendency, Stagge et al. (2017) observed, for the European continent in the period 1958–2014, that droughts were mainly driven by a temperature rise with the inherent increase in the evapotranspiration rate, whereas rainfall did not change appreciably. In the southwestern United States, Ting et al. (2018) found that, under a CO_2 warming scenario, earlier spring drying was mainly due to a decreased mean moisture convergence. A "flash"

drought occurring suddenly is frequently triggered by high temperatures or by severe water deficits (Wang and Yuan, 2018). Under the influence of global warming, a hypothesis has been formulated in which dry regions will tend to become drier while wet regions will tend to become wetter, the DDWW paradigm. Nevertheless, Yang et al. (2019) have observed that, on the global scale, this paradigm is mainly confirmed in precipitation-driven drought, when the plant and soil conditions are not considered.

One additional problem of drought is that it can spread towards other regions, as Herrera-Estrada et al. (2017) discovered in their Lagrangian analysis in several Earth regions. Andreadis et al. (2005) have elaborated on severity-area-duration maps, modifying an earlier proposal of Dalezios et al. (2000) for severity-duration-frequency maps. Therefore, drought is a present-day risk at least for a part of our society.

Drought characterization depends on the perspective of the user. The meteorological drought is possibly the simplest type to evaluate since it is reduced to a mere consideration of the rainfall. The two main meteorological drought indices are those mentioned above, the PDSI and SPI. Hydrological drought requires the conversion of rainfall into runoff, which can be done with the help of a hydrological model; the SPEI, for instance, is a widely used hydrological drought index. Nevertheless, Van Loon and Van Lanen (2012) have explored in depth the definition of hydrological drought, starting from the time perspective of the phenomenon, and distinguishing several types in terms of the sequences rain to snow, wet to dry, cold snow and warm snow seasons and what they denominated as classical rain deficit. The use of a simple hydrological model and the establishment of some threshold values allow Van Loon and Van Lanen (2012) to determine the drought occurrence in several regions with distinct climate types. Drought severity is a function of the available water storage units, as Van Loon and Laaha (2015) explained in the review of an Australian dataset. Hobbins et al. (2016) have modified the SPEI index by representing the potential evapotranspiration and the atmospheric evaporative demand on a proper physical basis, rather than on the air temperature as a proxy of it. Their evaporative demand drought index (EDDI) is a useful indicator of drought extent, as was shown by McEvoy et al. (2016) in the conterminous US. The estimation of the agricultural drought index is somewhat similar to that of the hydrological drought one, with the additional complexity of crop behavior. Several models have been proposed for the agricultural drought index estimation. As Perrin et al. (2001) warned, and Orth et al. (2015) later confirmed, the models set up to describe soil water evolution for this purpose must be very simple and limited to soil water balance. Hunt et al. (2009), Khare et al. (2013) and Sohrabi et al. (2015) proposed reasonable soil water balance models, differing only in their characterizations of rainfall infiltration, in order to prevent the generation of excess rain, deep percolation and actual evapotranspiration rate.

The different drought indices represent distinct aspects of drought. Therefore, to gain a wider perspective, Kao and Govindaraju (2010) introduced the use of copulas in a new drought indicator denominated the joint deficit index (JDI), based on the SPI for both precipitation and streamflow. Hao and AghaKouchak (2013) formulated another copula, the multivariate standardized drought index (MSDI), consisting of the SPI and a standardized soil moisture index (SSI). This index was very useful for detecting the drought onset and duration. Alternatively, Zarch et al. (2015) used two separate indices to assess droughts, the SPI and the reconnaissance drought index (RDI). A different approach was suggested by Hao et al. (2017) with a categorical drought prediction model, the U.S. Drought Monitor (USDM), which proved to be highly adequate for early warning. Azmi et al. (2016) developed a data fusion-based drought index, grouping different indices with a clustering method.

The impact of drought on vegetation can be by means of several indices. Kogan (1995) proposed a vegetation condition index (VCI) based on the normalized difference vegetation index (NDVI), which is a good indicator of vegetation status, by combining the radiance of the visible and infrared wavelengths to assess the drought effects. Some other indices have been suggested, since NDVI is sometimes influenced by other environmental factors (Quiring and Ganesh, 2010). The normalized difference water index (NDWI) was introduced by Gao (1996), and, using radiances in a higher wavelength range than that of NDVI, it is less affected than the latter by atmospheric conditions; it is also more sensitive to drought than other indices (Gulágsi and Kovács, 2015). The Joint Research Centre of the European Comission uses the fraction of absorbed photosynthetically active radiation (fAPAR) generated from the signals acquired by the Project for On-Board Autonomy - Vegetation (PROBA-V) sensor.

The abovementioned methods can be used to evaluate the impact of drought on agricultural productivity in regions worldwide, as Sepulcre-Cantó et al. (2012) have shown for Europe. These authors proposed a combined drought indicator using SPI, fAPAR and soil moisture calculated from a regional hydrological model. For the management of local policy and mitigation actions, such as farm-scale insurance schemes, smaller spatial scales than those used by Sepulcre-Cantó et al. (2012) are required.

The main objective of this work is to assess agricultural drought by means of a combined drought indicator (CDI), based on SPI and anomalies in soil moisture and NDVI. This new CDI is thus related to crop damage data in rainfed wheat-producing regions in southern Spain at the agricultural province level, which corresponds to the most important item of available yield data. It is expected that this new CDI will be useful at the local policy level and for planning farm-scale insurance schemes.

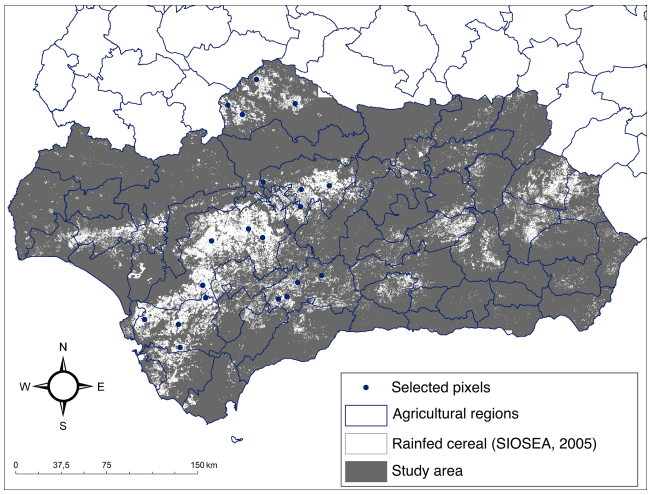

Figure 1. Location of the study area (grey) and selected representative points (blue dots) within the areas cultivated with cereal (white).

2 Materials and methods

2.1 Study area

This study was made in Andalusia, southern Spain, during the 10-year period between 2003 and 2013.

Andalusia has a Mediterranean climate with dry, hot summers (Köppen-Geiger climate Csa, Peel et al., 2007). Since the main source of water is rain caused by the western and southwestern winds carrying moist air from the Atlantic Ocean, the distribution of precipitation is conditioned by the orography of the region, with a main decreasing gradient from west to east.

The effect of drought on agricultural production was evaluated in five representative areas, in each of which, four representative locations were selected in a two-step procedure. First, the distribution of the land use class "non irrigated arable land" within the study area was analyzed, as shown in Fig. 1. This land use distribution is derived from the regional land use map (SIOSE: Soil Occupation Information System of Spain) applied to Andalusia, 2005, equivalent to the European CORINE database, on a scale of 1 : 10 000. This class occupies 20 %, 886 250 ha, of the total agricultural area occupied in Andalusia, 4 402 760 ha (Censo Agrario, 2009). Although the non-irrigated arable land class also includes other noncereal crops, in our study area wheat is by far the dominant crop. Five agricultural districts in Andalusia were selected where it is the leading crop: Campiña de Cádiz (Cádiz), Campiña Baja (Córdoba), Pedroches (Córdoba), Norte/Antequera (Málaga) and La Campiña (Sevilla). In each of these districts, four representative point locations were selected, yielding a total of 20 point locations. These point locations correspond to pixels that have a resolution of 250 m × 250 m, equivalent to the resolution of the NDVI imagery (see Sect. 2.4). These pixels were carefully selected and subjected to a visual case-by-case analysis in order to exclude anomalies and ensure a homogeneous land use in the following remote sensing analysis. Each of the 20 point locations had to fulfill the following conditions that were checked manually using aerial orthophoto imagery from 2004 to 2013:

i. It contains homogeneous land use of rainfed wheat within each pixel (with no other land uses present in it);

ii. It lacks external landscape elements, such as ponds, roads, canals, houses or natural vegetation patches that could distort the NDVI signal;

iii. It has continuous wheat cultivation during the study period (no fallow period).

2.2 Standardized precipitation index (SPI)

The SPI expresses the deviation of rainfall from its long-term mean. SPI is calculated by fitting the precipitation data to a gamma distribution, after which it is transformed into a normal distribution. The SPI values can then be interpreted as representing the number of standard deviations by which the observed anomaly deviates from the long-term mean. SPI was calculated over 1-, 3- and 6-month periods, using precipitation series of between 42 and 69 years, namely SPI-1, SPI-3 and SPI-6.

SPI-1 is theoretically best related to meteorological drought, together with short-term soil moisture stress, especially in periods when crop growth is sensitive to them (Guttman, 1999). SPI-3 has been shown to reflect short to medium seasonal precipitation trends (Guttman, 1999). Bussay et al. (1999) and Szalai and Szinell (2000) evaluated the relationship between SPI and agricultural drought through soil moisture and found that SPI-2 and SPI-3 yielded the best results. Other authors (Ji and Peters, 2003; Rossi and Niemeyer, 2012) have reported a high correlation between SPI-3 and vegetation response and, therefore, deemed this index to be the best suited for evaluating agricultural drought. They deemed SPI-6 to be the best one for identifying longer-term or seasonal drought trends.

The program "SPI_SL_6.EXE", developed by the National Drought Mitigation Center, University of Nebraska-Lincoln, was used to calculate SPI. Details of this method can be found in McKee et al. (1993) and Lloyd-Hughes and Saunders (2002). The same classification used by McKee et al. (1993) was used (Table 1), and a threshold value for defining a drought of SPI > -1.00 was employed following Cancelliere (2004).

SPI values were calculated for each of the five agricultural regions selected: Campiña de Cádiz (Cádiz), Campiña Baja (Córdoba), Pedroches (Córdoba), Norte/Antequera (Málaga) and La Campiña (Sevilla). The climate series selected in each

Table 1. Classification of droughts according to SPI and their probability of occurrence following McKee et al. (1993)

SPI	Category	Probability (%)
≥ 2.00	Extremely wet	2.3
1.50 to 1.99	Severely wet	4.4
1.00 to 1.49	Moderately wet	9.2
0.00 to 0.99	Mildly wet	34.1
0.00 to −0.99	Mild drought	34.1
−1.00 to −1.49	Moderate drought	9.2
−1.50 to −1.99	Severe drought	4.4
≤ -2	Extreme drought	2.3

region was the one at their particular weather station that had the longest available series.

2.3 Soil moisture anomaly index (SMAI)

The deviation of the soil moisture from its long-term mean was expressed as a soil moisture anomaly index (SMAI). SMAI values were calculated for each of the five selected agricultural regions, similar to those of the SPI. To obtain this index, we first calculated soil moisture dynamics by means of the simple water balance model of Brocca et al. (2008). The long-term mean soil moisture was taken as the 10-year mean in the study period (2003–2013). In this water balance model, the water depth in the soil profile, W, evolves with time, t, following the contribution of the infiltration of the rain, f, and the extraction of the evapotranspiration, e, and of the deep percolation or of the surface and subsurface runoff, g. The balance was computed on the daily timescale following Eq. (1):

$$\frac{\mathrm{d}W(t)}{\mathrm{d}t} = f - e - g. \tag{1}$$

The infiltration depth is estimated from the rain depth, p, the wetness or relative soil water content, normalized by the maximum value, $W_{\max}$, $\omega = W/W_{\max}$ and a parameter m, with the empirical approximation proposed by Georgakakos (1986), using Eq. (2):

$$f = p\left(1 - \omega^m\right). \tag{2}$$

The deep percolation or runoff loss is estimated by a simple potential function with the saturated hydraulic conductivity, k_s, and λ, the pore size distribution index of Brooks and Corey (1966) using Eq. (3):

$$g = k_s \omega^{3+2/\lambda}. \tag{3}$$

Finally, the daily evapotranspiration rate is estimated as the FAO Penman–Monteith (Allen et al., 1998) potential rate, e_0, modified by the wetness, using Eq. (4):

$$e = \omega e_0. \tag{4}$$

Table 2. Parameters for the water balance model used in this study.

Parameter	Value	Source
m (–)	10	mean value of the interval proposed by Brocca et al. (2008).
$W_{\max}$ (mm)	175	as proposed by Vanderlinden (2001) in a study based on a soil map of Andalusia.
k_s (mm d^{-1})	38.4	estimate of soil water properties by Rawls et al. (1998); representative value for clay loam according to USDA classification.
λ (–)	0.15	derived from graphs of the parameter λ in Brooks and Corey (1966) as a function of soil texture, organic matter content and increase in soil porosity above the reference value (Rawls et al., 1983).

The parameter values adopted here are shown in Table 2.

The soil moisture anomaly index (SMAI) is then given by Eq. (5):

$$\mathrm{SMAI} = \frac{W - \overline{W}}{\sigma_W}, \tag{5}$$

where $\overline{W}$ is the long-term average soil moisture and σ_W its standard deviation.

2.4 NDVI anomaly index (NDVIA)

Different agricultural drought studies have used satellite-based vegetation indices as their main advantage is their spatial and temporal resolution. NDVI values represent the plant chlorophyll content, which is why they are highly suitable for identification of agricultural drought. Limitations in its use are related to the fact that NDVI may reflect non-drought-related stress conditions, such as plant disease, and that soil properties can induce a bias in its response. Therefore, it is important to use NDVI-based drought evaluation in combination with other indices based on precipitation or soil water, as is the case here. NDVI anomalies express deviations in NDVI from its long-term mean, and these were evaluated on a monthly basis but only taken into account from November to April, which is the normal growing season for rain-fed winter cereal in Andalusia. Only during this period can NDVI and its anomalies be expected to transmit information on rain-fed cereal growth. The long-term mean NDVI was taken as the 10-year mean in the study period (2003–2013).

Thanks to its spatial continuity, NDVI trends could be analyzed for 20 different points; i.e., four points or pixels were analyzed in each of the five agricultural regions selected. This analysis yielded a total of 20 spatially different NDVI anomaly indices. The NDVI anomaly index was calculated

using Eq. (6):

$$\text{NDVI anomaly index} = \frac{\text{NDVI}_i - \overline{\text{NDVI}}}{\sigma_{\text{NDVI}}}, \quad (6)$$

where NDVI_i, $\overline{\text{NDVI}}$ and σ_{NDVI} are, respectively, its value at a particular moment in time, its long-term mean value and its standard deviation. NDVI data were derived from Terra MODIS (moderate resolution imaging spectroradiometer) that collects imagery for each point on Earth every 1–2 d. Based on these data, a monthly average was calculated and used for NDVI_i (Department of Agriculture, Fisheries and Environment, Government of Andalusia). For each of the five regions, the final NDVIA index was then calculated based on the average of the four points or pixels of that region.

2.5 Combined drought indicator (CDI)

The main idea behind the combined drought indicator (CDI) for identifying agricultural drought is an idealized cause–effect relation between water deficit and yield. There are different phases in this relationship: a precipitation deficit (phase 1) leads initially to soil water deficit (phase 2), which, if prolonged over time, will result in crop water stress and be reflected in the NDVI observed (phase 3), which finally generates a reduction in cereal yields (phase 4).

In its simplest form, this CDI would allow us to identify which cause–effect relationship phase the agricultural system has reached in the event of a drought. This indicator would then allow the establishment of a series of drought warnings, depending on that phase. The CDI should be seen as a first step towards designing that warning system.

This study proposes a CDI that combines three indices:

- SPI-3 to identify the first level of precipitation deficit (phase 1)
- SMAI to identify anomalies in the soil moisture (phase 2)
- NDVI anomalies to characterize the subsequent effect of soil water stress on crops (phase 3).

The warning levels suggested for the CDI proposed are given in Table 3. They aim and are expected to help policy makers to prepare and take action in the case of droughts.

The CDI uses three different levels; the first two, watch and warning, indicate that a drought could be imminent. The highest level of the CDI is "alert". The two types of alert include those cases in which a meteorological drought results in a rapid yield decrease. The type I alert can occur even without a previous anomaly in soil moisture values, which could be related to intense droughts occurring during sensitive phenological phases of the crop. Therefore, a type I alert depends on only two indicators, SPI-3 and NDVI. The type II alert is based on all three indicators composing the CDI (SPI-3, SMAI and NDVI) so that these give firmer evidence for the existence of an agricultural drought.

2.6 Insurance data

The insurance area data and those of areas affected by drought per agricultural season for rainfed cereal were given by Agroseguro, the Spanish agricultural insurance provider. These data were disaggregated for each area of the five under study and each agricultural season, from 2002–2003 to 2011–2012. Note that data for the last year of the study, 2012–2013, were not provided. Crop intensity damage is expressed as the percentage of surface area that was filed for damage with respect to the total insured area and is available on an agricultural region scale. Crop damage of close to 100 % indicates important losses during that year.

3 Results

3.1 SPI

The SPI values calculated over a 3-month period (SPI-3) reflected short–medium term moisture conditions and provided an estimate of the seasonal precipitation that was useful for agricultural purposes. In our study area, defined in Sect. 2.1, SPI-3 values at the end of April revealed the precipitation trends during the plant reproduction stage and the grain development. SPI-3 at the end of December showed moisture conditions at the start of the growing season.

Figure 2 gives the trends in SPI-3 for all five selected agricultural regions. The trends are similar in all regions, with SPI-3 values moving periodically around the long-term mean or 0 value. In the driest years, one can observe the highest negative peaks. For example, during the agricultural year 2004–2005, which was very dry, negative values of up to -2.50 can be observed for Campiña de Cádiz, indicating the drought severity. Another dry year was 2011–2012, when values of up to -2.12 could be observed during the month of February in La Campiña. So, clearly, the two main dry periods were correctly identified by the trends in SPI. However, this drought indicator also defined other different periods that were not markedly dry as being critical. In 2008–2009 all the regions are distinguished for being critical SPI levels, albeit for short periods of time and mainly towards the summer or end of the agricultural year. Even in 2012–2013 critical drought periods were flagged in four out of five regions.

3.2 SMAI

Figure 3 shows the variation in the SMAI over the period studied and for each of the five agricultural regions. The two main dry periods of 2004–2005 and 2011–2012 are not consistently apparent. Generally, only two regions at that time dipped below the -1 mark and are indicated in red: (a) Campiña de Cádiz and (d) Norte/Antequera for 2004–2005 and (a) Campiña de Cádiz and (b) Campiña Baja for 2011–2012. The year 2007–2008 seems to be marked by drier soil water contents compared to the long-term mean, as

Table 3. Classification of the combined drought indicator (CDI).

Level	Definition			C: characteristics, S: situation, A: actions
	SPI-3	SMAI	NDVIA	
Watch	<-1			C: relevant precipitation deficit observed S: probability of agricultural drought occurring A: surveillance of the situation and preparation for actions
Warning	<-1	<-1		C: relevant precipitation deficit translates into an anomaly (deficit) in soil moisture S: agricultural drought expected A: activate response strategies for minimizing drought exposure
Alert type I	<-1		<-1	C: precipitation deficit is accompanied by an anomaly in vegetation condition and precipitation deficit leads to water stress in cereal S: agricultural drought has started to affect yield negatively A: fortification of response strategies and careful follow up of the situation
Alert type II	<-1	<-1	<-1	C: precipitation and soil moisture deficit are accompanied by anomalies in the vegetation condition, such as water stress in cereal after precipitation and soil moisture deficit S: agricultural drought has started to affect yield negatively A: fortification of response strategies and careful follow up of the situation

critical levels are reached for four out of the five agricultural regions.

3.3 NDVIA

Figure 4 shows a map indicating the spatial and temporal variability in NDVI values over Andalusia for the year 2004. Figure 4a indicates NDVI in April, right in the growing season, while Fig. 4b shows the same area after the cereal has been harvested. The color red indicates low values of NDVI, while green represents maxima of between 0.96 in April and 0.92 in June. When comparing the distribution of the main cereal-growing regions in the area in Fig. 1, these areas present the most important variation between the two images, with high values in April and low red ones in June.

Figure 5 shows the monthly variation in the NDVI anomaly for the four selected pixels within the Campiña agricultural region. The pixels in the other four agricultural regions are not shown, but their trend is similar. There is, of course, an important spatial variability within the area, such that some differences appear between the four study locations. This can be attributed to different planting dates, crop varieties or soil properties between the locations. Over the study period, however, the same general temporal trends appear. Important negative deviations from the mean indicate periods of high plant stress. Values of NDVI anomaly below -1 are marked in red. Its evolution is similar to that of SPI-3 and SMAI (Figs. 2 and 3), although there is clearly a time lag effect. Plant stress generally only occurs after precipitation and a deficit in soil moisture. Also, the temporal pattern is more erratic than in the case of SPI-3 and SMAI. However, the previously mentioned 2004–2005 and 2011–2012 droughts can be identified as being the negative peaks in Fig. 4. During other years, isolated red deviations appear, but these are not generalized among all four sites. The only exception is 2008–2009, when a generalized NDVI anomaly appears in all of them, but it occurs early during the first months of the growing season, so perhaps it can be attributed to a late seeding that year.

3.4 CDI

Figure 6 shows the monthly evolution of CDI between 2003 and 2013 and compares its levels against crop damage data derived from agricultural insurance information. This occurs twice during the studied period on a regionalized scale, indicating the effects of a drought. The first time is during the agricultural year 2004–2005, with losses of between 73 % and 99 % in the five agricultural regions studied. Also, for the years 2011–2012, there was considerable crop damage of between 71 % and 92 %. A third season, 2009–2010, had medium to high losses, of between 44 % and 89 %. However, crop damage during this period is, rather, due to the effects of excessive precipitation, leading to water stagnation and erosion damage. This can be seen when comparing the annual precipitation values. For example, in the Córdoba agricultural region, with a mean long-term precipitation of 600 mm, the values for 2004–2005, 2009–2010 and 2011–2012 are, respectively, 423, 1179 and 433 mm.

The CDI accurately captured these two important drought periods. For the first area, Campiña de Cádiz (Fig. 6a), a series of drought warning levels were issued early in the agricultural year 2004–2005, followed by a type I alert in January. There was another type I and II alert in May–June. In

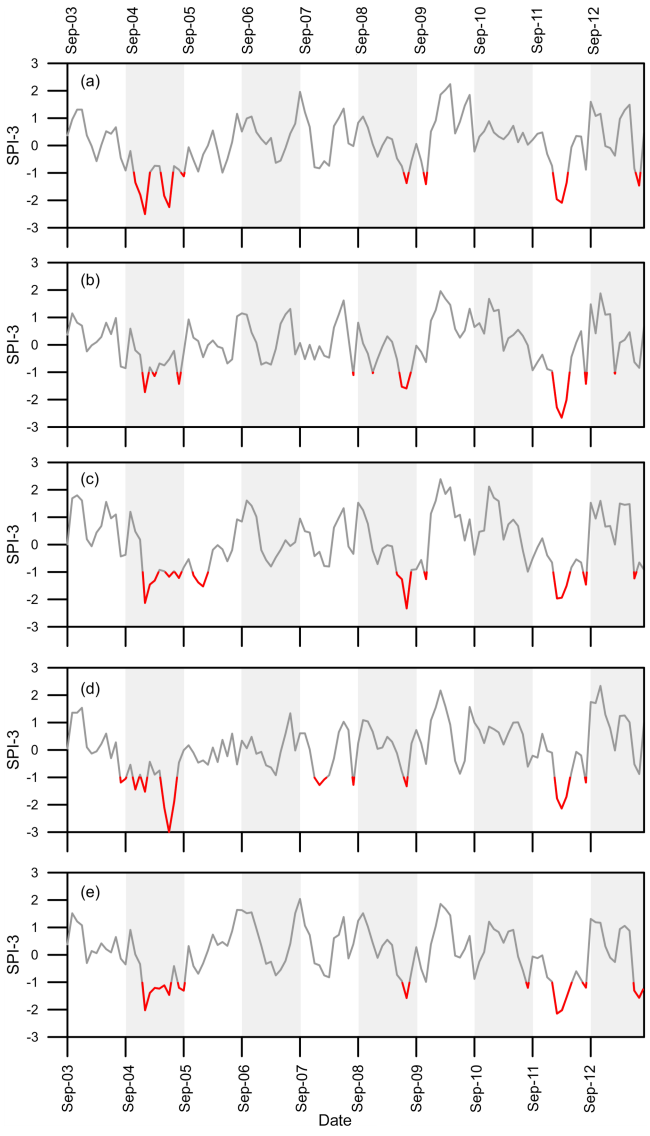

Figure 2. Variation of the standardized precipitation index over 3 months (SPI-3) during the period studied (2003–2013) in the five selected agricultural regions: **(a)** Campiña de Cádiz, **(b)** Campiña Baja, **(c)** Pedroches, **(d)** Norte/Antequera and **(e)** La Campiña. Red lines indicate values below the defined threshold of −1.

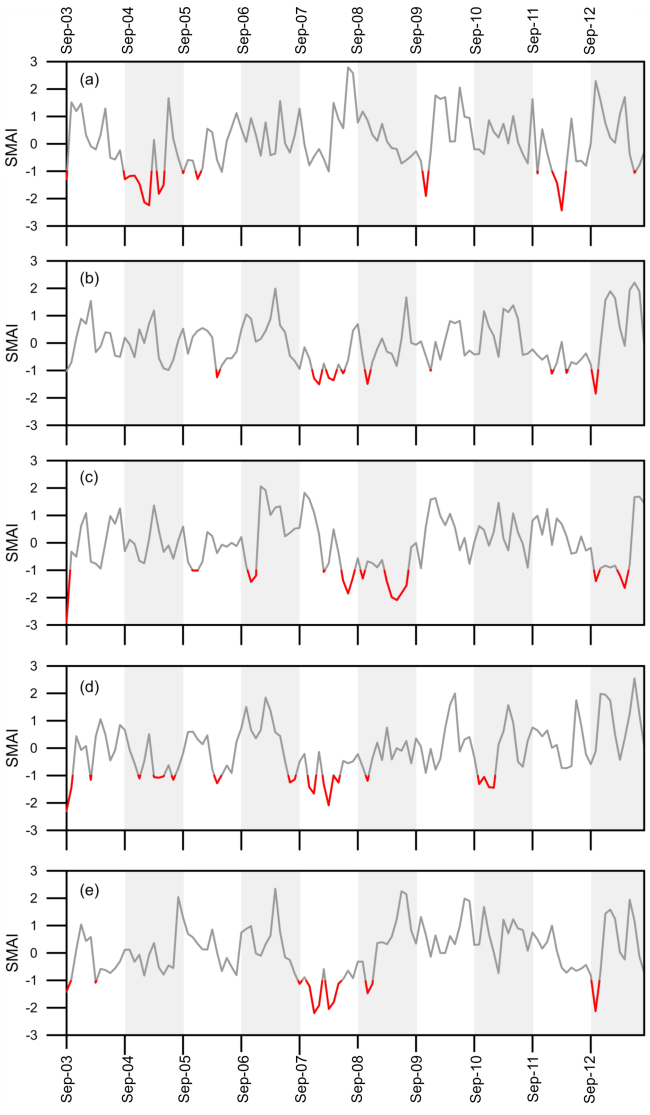

Figure 3. Variation of the soil moisture anomaly index (SMAI) during the period studied (2003–2013) in the five selected agricultural regions: **(a)** Campiña de Cádiz, **(b)** Campiña Baja, **(c)** Pedroches, **(d)** Norte/Antequera and **(e)** La Campiña. Red lines indicate values below the defined threshold of −1.

other words, since the seeding and during the first months of crop growth, there was a continued series of drought warnings or alerts. In that particular year, 90 % of the insured area was reported as being damaged. In 2005–2006, the CDI registered another warning indication, but it did not lead to any damage to the crop. In September 2005 there was a type II alert, but that month is outside the cereal growth period and when the crop was seeded two months later, the situation had gone back to normal. In May 2006 another warning was issued due to a precipitation and a soil moisture deficit. However, the crop was already at the moment in its cycle when it was close to harvesting and it was therefore not affected so much. In 2009–2010, characterized by considerable crop damage, 89 % of the total insured area, there was only one alert, in November. As mentioned before, crop damage during that season was probably due to precipitation excess rather than drought. For the dry period of 2011–2012, the CDI accurately indicated that critical situation with a warning, followed by type I and II alerts in the period of February–April.

For the Campiña Baja region (Fig. 6b) the dry period of 2004–2005 was characterized by a continuous series of type I and II alerts from January to June, with two more alerts during the summer, outside the cereal growing period. In this region, the insured area damaged that year was also very ex-

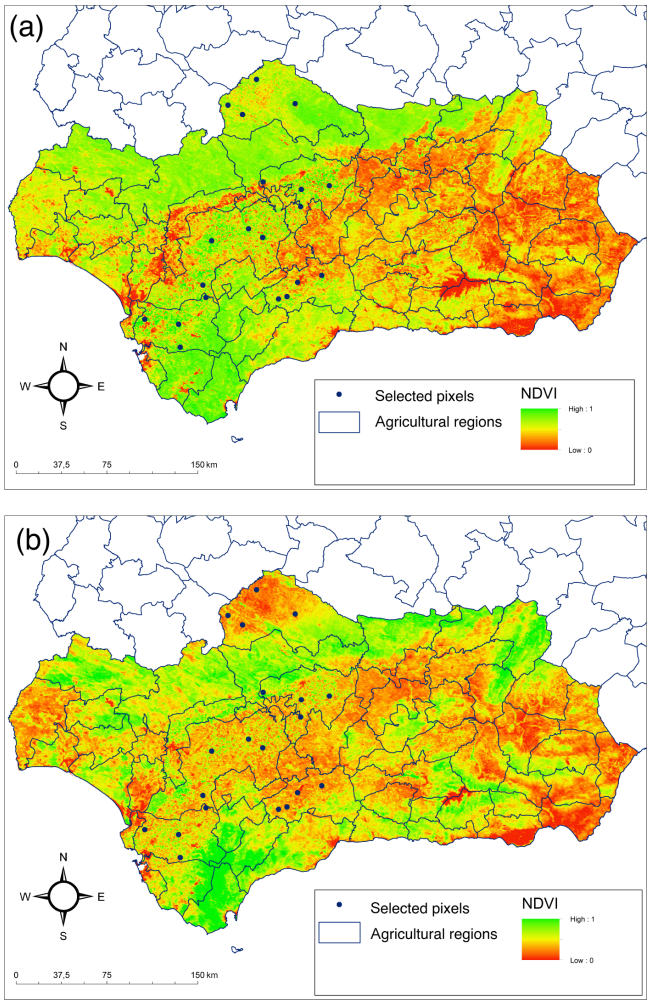

Figure 4. NDVI values all over Andalusia in **(a)** April 2004 and **(b)** June 2004. Important changes from green to red are observed in the main grain-growing areas, while areas with natural forests and shrubs remain green. Blue dots show the four representative pixels that were selected within each of the five agricultural regions studied.

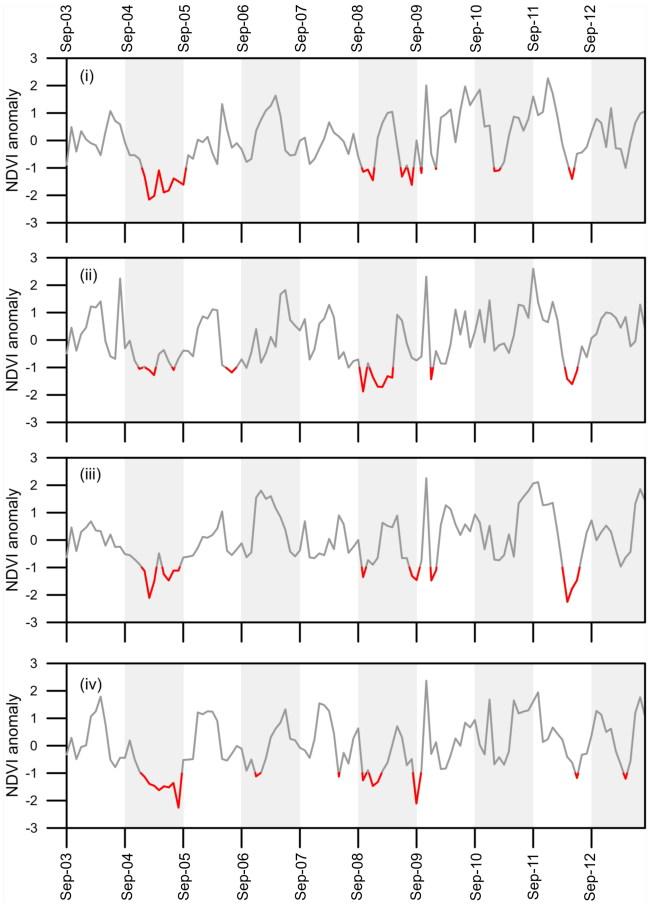

Figure 5. Variation of the monthly NDVI anomaly for the four selected locations within the region "La Campiña" over the study period. Red lines indicate values below the defined threshold of −1.

tensive (95 %). In 2008–2009 a warning was issued that did not cause any yield losses, as only 15 % of the insured area was damaged. This can be explained by the fact that this situation did not occur at a time when the crop was sensitive. In another dry year, 2011–2012, a series of warnings were issued, from January to March, followed by, respectively, type II and I alerts in April and May. These all occurred at times when the crop was highly sensitive, so that it was seriously damaged in 90 % of the area.

In the Pedroches region (Fig. 6c), the two main dry periods were well predicted. The year 2004–2005 was distinguished by a series of type II alerts in January, February, March and May and a type I alert in June. This sequence of critical CDI levels was reflected in an insured crop area with 73 % of damage. In 2005–2006, although there were two types of stress situations, warnings and type II alerts from November to February, the damage rate was not a high one, only 15 % of the insured area. It is difficult to understand the underlying reasons for the good performance of the crop that year. For example, during the years 2008–2009, the incidents were clearly late in the year (May to July), a period when grain growth is not sensitive. The second dry period of 2011–2012 is marked by a number of type II alerts issued from February to April, at a time when the cereal is highly vulnerable. This is reflected in a 71 % damaged insured area.

In the Comarca Norte/Antequera region (Fig. 6d), the dry period of 2004–2005 was determined by several incidents early on, with a watch issued in November and a type II alert in January, the latter being the period of cereal nascence and other sensitive growth stages. That year, the damaged insured area was 88 %. In 2007–2008 there were two warnings and a type II alert, from December to February, but these did not lead to crop damage, as the damaged insured area was only 11 %. Again, the reason could be found in those droughts occurring during a period when the cereal was not too sensitive. During the second main dry period of 2011–2012, a

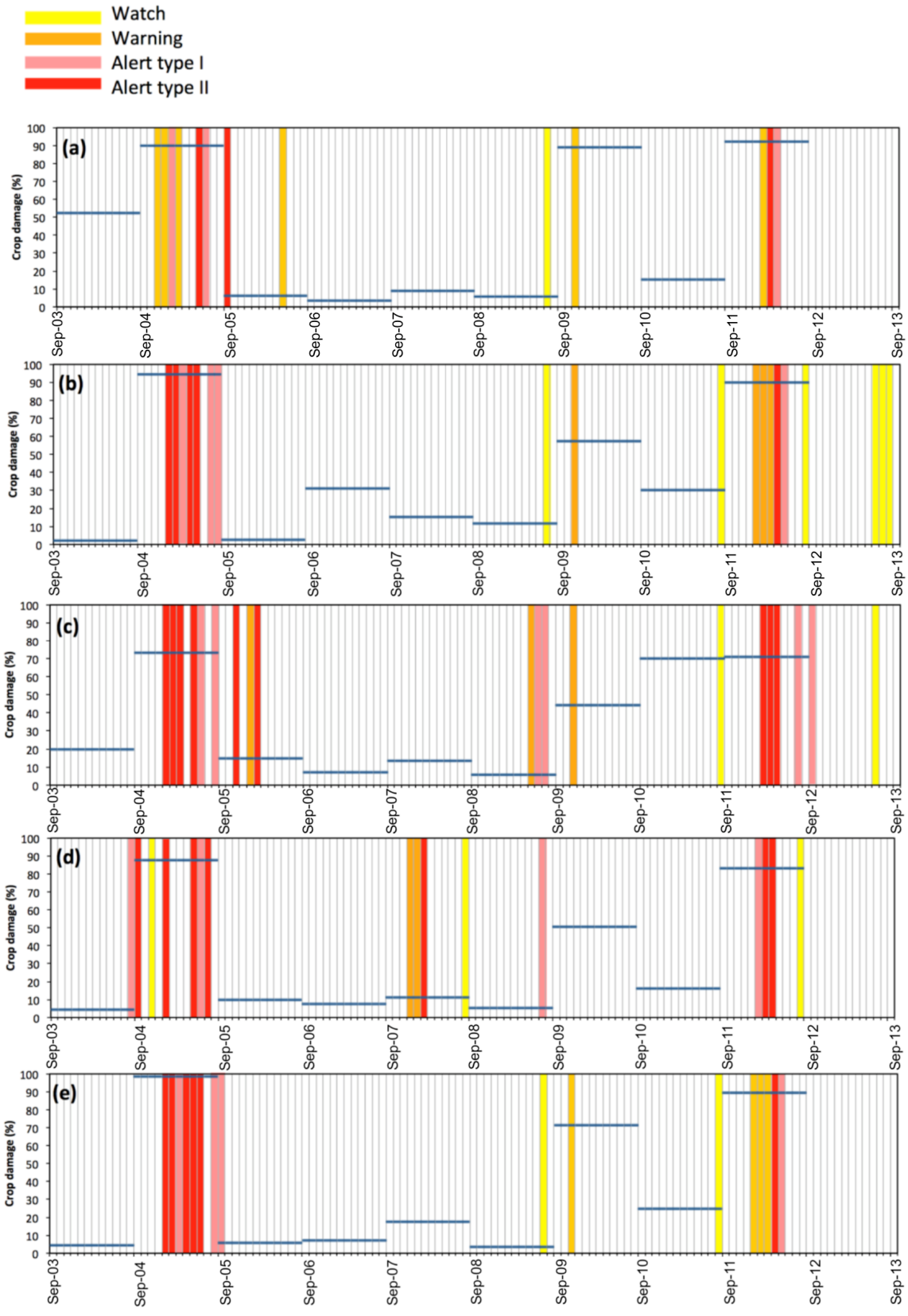

Figure 6. Evolution of the combined drought indicator (CDI) from 2003–2013 and comparison with agricultural crop damage intensity (blue lines) for the five agricultural regions studied: **(a)** Campiña de Cádiz,**(b)** Campiña Baja, **(c)** Pedroches, **(d)** Norte/Antequera and **(e)** la Campiña.

number of type I and II alerts were issued between February and April. These corresponded to highly sensitive moments of the crop cycle, and damaged insured areas were consequently high that year, amounting to 83 %.

The last region, La Campiña (Fig. 6e), showed a similar trend, with 2004–2005 being identified as having an extremely high damaged insured area of 99 %. The CDI worked well in predicting this, as there were multiple and continued alerts; i.e., from January to June there was a continued type II alert, except in March when it was a type I alert. In 2009–2010 there was a watch in November, and the damaged area was 72 %. However, as mentioned before, the absence of any further drought watches during that year and the high total annual rainfall indicate that the damage was likely to have been caused by excess precipitation. In the second main dry period of 2011–2012, the situation was worse, with a number of warnings from January to March, a type II alert in April and again a type I alert in May. That year the damaged insured area was high, up to 90 %.

4 Discussion

The results led to the conclusion that the performance of the newly proposed CDI is adequate (Fig. 6). The periods of high crop damage – between 70 and 95 % – in the two important dry periods of 2004–2005 and 2011–2012 were accompanied by watches, warnings and type I or II alerts of CDI in the five agricultural regions studied. This combined indicator has several advantages over using a single one, as is evidenced by the trends in precipitation, soil moisture and vegetation alone. Soil moisture, for example, did not include the two main dry periods, 2004–2005 and 2011–2012, in all of the areas. The soil moisture anomaly index only indicated drought in two out of five regions for each of these dry periods, and this could probably be improved by measurements of in situ soil moisture. Krueger et al. (2017), for example, showed how in situ soil moisture measurements explained wildfire incidence much better than the widely used Keetch–Byram drought index (KBDI). Like our SMAI, the KBDI is a drought index calculated on a daily scale, but it only considers daily temperature and precipitation in calculating soil moisture. Whereas our SMAI uses a more advanced soil water balance algorithm (using variable infiltration rates and refining the estimation of the actual evapotranspiration rate from the potential rate computed by the FAO-Penman Monteith equation), and it is clear that future studies should focus on site-specific calibrations of soil moisture dynamics against field data or by observations from remote sensing. Martínez-Fernández et al. (2015) successfully applied in situ soil moisture measurements to predict agricultural droughts in northern Spain. Other studies, like that of Kędzior and Zawadzki (2017), have used SMOS-derived soil moisture anomalies. They concluded that these were suitable for calculating agricultural drought risk in the Vistula river catchment. Another possibility for improving drought prediction based on soil moisture is to combine different models. Cammalleri et al. (2016) used joint means from three different models, LISFLOOD, CLM and TESSEL, and were able to increase the correlation with observations and reduce the number of false drought alarms.

In any case, our results corroborate previous studies using combined indicators that also concluded that they yielded good results for agricultural drought prediction. Sepulcre-Canto et al. (2012), for example, use a similar CDI, based on SPI, soil moisture and photosynthetically active radiation (fAPAR). They evaluate this indicator on the continental scale and assess its performance against annual cereal yield at the regional level. They conclude that their indicator is successful in predicting drought periods and lower yields. While our indicator is similar in conception, there are notable differences with the CDI proposed in this study, firstly in the way soil moisture anomalies are calculated and secondly by using NDVI instead of fAPAR. Gouveia et al. (2009), comparing a soil water index against NDVI response in Portugal, found a good correlation between NDVI and soil water content under different land use conditions. They concluded that NDVI values of arable land were more sensitive to drought compared to forests, which suggests that NDVI is particularly well suited in this study of cereal growing areas.

Future studies could focus on improving this combined indicator, for example by using other probability density functions rather than the gamma function used for calculating the SPI. Sienz et al. (2012) obtained a better fit to precipitation data of several world regions with the Weibull rather than with the gamma probability distribution function. Carrão et al. (2016) selected an empirical standardized soil moisture index, which was highly correlated ($r^2 = 0.82$) with their maize–soybean and wheat yields in three study sites in Argentina.

5 Conclusions

This study has presented a new combined drought index (CDI) for the assessment of agricultural drought. This CDI uses a combination of anomalies in precipitation (SPI-3), soil moisture and NDVI. The alert results are classified in four levels ranging from watch, warning to alert (type I and II). The CDI dynamics have been assessed for a 10-year period between 2003 and 2013, characterized by two important drought periods (2004–2005 and 2011–2012), in the five main rainfed cereal-growing regions of SW Spain. Comparison with yield data shows that both dry periods, characterized by a high crop damage extent of between 70 % and 95 %, were correctly identified by different critical CDI levels in all five study regions. This demonstrates the potential of this CDI. Further research should focus on a better representation of soil moisture data, either by improving data input from in situ measurements or by remote sensing, or by using model

ensembles. Also, phenological information could be used to improve the performance of this indicator.

Data availability. Data are freely available upon request by contacting the corresponding author by email.

Author contributions. JVG and AT conceptualized the research goals. MdPJD collected the remote sensing data and performed the data analysis. MdPJD developed the paper with contributions from all coauthors.

Competing interests. The authors declare that they have no conflict of interest.

Special issue statement. This article is part of the special issue "Remote sensing, modelling-based hazard and risk assessment, and management of agro-forested ecosystems". It is not associated with a conference.

Acknowledgements. María del Pilar Jiménez-Donaire was supported by a CEIGRAM fellowship. The insurance data were kindly supplied by Agroseguro. Ana Tarquis is grateful to the Community of Madrid (Spain) and Structural Funds 2014-2020 (ERDF and ESF) for the financial support (project AGRISOST-CM S2018/BAA-4330 and EU project 821964, BEACON).

Financial support. This research has been supported by the European Commission, Horizon 2020 Framework Programme (BEACON (grant no. 821964)) and the Ministerio de Ciencia e Innovación (grant no. AGRISOST-CM S2018/BAA-4330).

Review statement. This paper was edited by Jonathan Rizzi and reviewed by three anonymous referees.

References

Allen, R. G., Pereira, L .S., Raes, D., and Smith, M.: Crop evapotranspiration: guidelines for computing crop water requirements, FAO irrigation and drainage paper. Food and Agriculture Organization of the United Nations, Rome, Italy, 1998.

Andreadis, K. M., Clark, E. A., Wood, A. W., Hamlet, A. F., and Lettenmaier, D. P.: Twentieth-Century Drought in the Conterminous United States, J. Hydrometeorol., 6, 985–1001, https://doi.org/10.1175/JHM450.1, 2005.

Azmi, M., Rüdiger, C., and Walker, J. P.: A data fusion-based drought index, Water Resour. Res., 52, 2222–2239, https://doi.org/10.1002/2015WR017834, 2016.

Brocca, L., Melone, F., and Moramarco, T.: On the estimation of antecedent wetness conditions in rainfall–runoff modelling, Hydrol. Process., 22, 629–642, 2008.

Brooks, R. H. and Corey, A. T.: Properties of Porous Media Affecting Fluid Flow, J. Irrig. Drain. E.-ASCE, 92, 61–90, 1966.

Bussay, A., Szinell, C., and Szentimery, T.: Investigation and Measurements of Droughts in Hungary, Hungarian Meteorological Service, New York, 1999.

Cammalleri, C., Micale, F., and Vogt, J.: A novel soil moisture-based drought severity index (DSI) combining water deficit magnitude and frequency, Hydrol. Proc., 30, 289–301, https://doi.org/10.1002/hyp.10578, 2016.

Cancelliere, A.: Drought length properties for periodic-stochastic hydrologic data, Water Resour. Res., 40, W02503, https://doi.org/10.1029/2002WR001750, 2004.

Carrão, H., Russo, S., Sepulcre-Canto, G., and Barbosa, P.: An empirical standardized soil moisture index for agricultural drought assessment from remotely sensed data, Int. J. Appl. Earth Obs., 48, 74–84, 2016.

Censo Agrario: National Institute for Statistics, available at: https://www.ine.es/dyngs/INEbase/es (last acess: 15 March 2019), 2009.

Cook, E. R., Seager, R., Kushnir, Y., et al.: Old World megadroughts and pluvials during the Common Era, Sci. Adv., 1, e1500561, https://doi.org/10.1126/sciadv.1500561, 2015.

Cook, B. I., Anchukaitis, K. J., Touchan, R., Meko, D. M., and Cook, E. R.: Spatiotemporal drought variability in the Mediterranean over the last 900 years, J. Geophys. Res.-Atmos., 121, 2060–2074, https://doi.org/10.1002/2015JD023929, 2016.

Dalezios, N., Loukas, A., Vasiliades, L., and Liakopoulos, E.: Severity-duration-frequency analysis of droughts and wet periods in Greece, Hydrolog. Sci. J., 45, 751–769, https://doi.org/10.1080/02626660009492375, 2000.

Gao, B.: NDWI – A Normalized Difference Water Index for RemoteSensing of Vegetation Liquid Water From Space, Remote Sens. Environ., 58, 257–266, 1996.

Georgakakos, K. P.: A generalized stochastic hydrometeorological model for flood and flash-flood forecasting. 1: Formulation, Water Resour. Res., 22, 2083–2095, 1986.

Gouveia, C., Trigo, R. M., and DaCamara, C. C.: Drought and vegetation stress monitoring in Portugal using satellite data, Nat. Hazards Earth Syst. Sci., 9, 185–195, https://doi.org/10.5194/nhess-9-185-2009, 2009.

Gulácsi, A. and Kovács, F.: Drought monitoring with spectral indices calculated from MODIS satellite images in Hungary, J. Environ. Geogr., 8, 11–20, 2015.

Guttman, N. B.: Accepting the Standardized Precipitation Index: a calculation algorithm, J. Am. Water Resour. As., 34, 113–121, 1999.

Hao, Z. and AghaKouchak, A.: Multivariate Standardized Drought Index: A parametric multi-index model, Adv. Water Resour., 57, 12–18, 2013.

Hao, Z., Yuan, X., Xia, Y., Hao, F., and Singh, V. P.: An overview of drought monitoring and prediction systems at regional and global scales, B. Am. Meteorol. Soc., 98, 1879–1896, 2017.

Herrera-Estrada, J. E., Satoh, Y., and Sheffield, J.: Spatiotemporal dynamics of global drought, Geophys. Res. Lett., 44, 2254–2263, https://doi.org/10.1002/2016GL071768, 2017.

Hobbins, M. T., Wood, A., McEvoy, D. J., Huntington, J. L., Morton, C., Anderson, M., and Hain, C.: The evaporative demand drought index. Part I: linking drought evolution to variations in evaporative demand, J. Hydrometeorol., 17, 1745–1761, 2016.

Hunt, E. D., Hubbard, K. G., Wilhite, D. A., Arkebauer, T. J., and Dutcher, A. L.: The development and evaluation of a soil moisture index, Int. J. Climatol., 29, 747–759, 2009.

Ji, L. and Peters, A. J.: Assessing vegetation response to drought in the northern Great Plains using vegetation and drought indices, Remote Sens. Environ., 87, 85–98, https://doi.org/10.1016/S0034-4257(03)00174-3, 2003.

Kao, S.-C. and Govindaraju, R. S.: A copula-based joint deficit index for droughts, J. Hydrol., 380, 121–134, https://doi.org/10.1016/j.jhydrol.2009.10.029, 2010.

Kędzior, M. and Zawadzki, J.: SMOS data as a source of the agricultural drought information: Case study of the Vistula catchment, Poland, Geoderma, 306, 167–182, https://doi.org/10.1016/j.geoderma.2017.07.018, 2017.

Keyantash, J. A. and Dracup, J. A.: The quantification of drought indices, B. Am. Meteorol. Soc., 83, 1167–1180, 2002.

Khare, Y. P., Martinez, C. J., and Muñoz-Carpena, R.: Parameter variability and drought models; a study using the agricultural reference index for drought (ARID), Agron. J., 105, 1417–1432, 2013.

Kogan, F. N.: Droughts of the Late 1980s in the United States as Derived from NOAA Polar-Orbiting Satellite Data, B. Am. Meteorol. Soc., 76, 655–668, 1995.

Krueger, E. S., Ochsner, T. E., Quiring, S. M., Engle, D. M., Carlson, J. D., Twidwell, D., and Fuhlendorf, S. D.: Measured Soil Moisture is a Better Predictor of Large Growing-Season Wildfires than the Keetch–Byram Drought Index, Soil Sci. Soc. Am. J., 81, 490–502, https://doi.org/10.2136/sssaj2017.01.0003, 2017.

Lloyd-Hughes, B. and Saunders, M. A.: A drought climatology for Europe, Int. J. Climatol., 22, 1571–1592, 2002.

Martínez-Fernández, J., González-Zamora, A., Sánchez, N., and Gumuzzio, A.: A soil water based index as a suitable agricultural drought indicator, J. Hydrol., 522, 265–273, https://doi.org/10.1016/j.jhydrol.2014.12.051, 2015.

McEvoy, D. J., Huntington, J. L., Hobbins, M. T., Wood, A., Morton, C., Anderson, M., and Hain, C.: The evaporative demand drought index. Part II:CONUS-wide assessment against common drought indicators, J. Hydrometeorol., 17, 1763–1779, 2016.

McKee, T. B., Doesken, N. J., and Kleist, J.: The relationship of drought frequency and duration to time scales, in: Proceedings of the 8th Conference on Applied Climatology, American Meteorological Society Boston, MA, 179–183, 1993.

Orth, R., Staudinger, M., Seneviratne, S. I., Seibert, J., and Zappa, M.: Does model performance improve with complexity? A case study with three hydrological models, J. Hydrol., 523, 147–159, 2015.

Peel, M. C., Finlayson, B. L., and McMahon, T. A.: Updated world map of the Köppen-Geiger climate classification, Hydrol. Earth Syst. Sci., 11, 1633–1644, https://doi.org/10.5194/hess-11-1633-2007, 2007.

Perrin, C., Michel, C., and Andréassian, V.: Does a large number of parameters enhance model performance? Comparative assessment of common catchment model structures on 429 catchments, J. Hydrol., 242, 275–301, https://doi.org/10.1016/S0022-1694(00)00393-0, 2001.

Quiring, S. M. and Ganesh, S.: Evaluating the utility of the Vegetation Condition Index (VCI) for monitoring meteorological drought in Texas, Agr. Forest Meteorol., 150, 330–339, 2010.

Rawls, W. J., Brakensiek, D. L., and Soni, B.: Agricultural Management Effects on Soil Water Processes Part I: Soil Water Retention and Green and Ampt Infiltration Parameters, T. ASAE, 26, 1747–1752, 1983.

Rawls, W. J., Gimenez, D., and Grossman, R.: Use of soil texture, bulk density, and slope of the water retention curve to predict saturated hydraulic conductivity, T. ASAE, 41, 983–988, 1998.

Rossi, S. and Niemeyer, S.: Drought Monitoring with estimates of the Fraction of Absorbed Photosynthetically-active Radiation (fAPAR) derived from MERIS, in: Remote Sensing for Drought: Innovative Monitoring Approaches, edited by: Wardlow, B. D., Anderson, M. C., and Verdin, J. P., CRC Press Boca Raton, FL, USA, 95–120, 2012.

Sepulcre-Canto, G., Horion, S., Singleton, A., Carrao, H., and Vogt, J.: Development of a Combined Drought Indicator to detect agricultural drought in Europe, Nat. Hazards Earth Syst. Sci., 12, 3519–3531, https://doi.org/10.5194/nhess-12-3519-2012, 2012.

Sienz, F., Bothe, O., and Fraedrich, K.: Monitoring and quantifying future climate projections of dryness and wetness extremes: SPI bias, Hydrol. Earth Syst. Sci., 16, 2143–2157, https://doi.org/10.5194/hess-16-2143-2012, 2012.

Sohrabi, M. M., Ryu, J. H., Abatzoglou, J., and Tracy, J.: Development of soil moisture drought index to characterize droughts, J. Hydrol. Eng., 20, 04015025, https://doi.org/10.1061/(ASCE)HE.1943-5584.0001213, 2015.

Stagge, J. H., Kingston, D. G., Tallaksen, L. M., and Hannah, D. M.: Observed drought indices show increased divergence across Europe, Sci. Rep.-UK, 7, 14045, https://doi.org/10.1038/s41598-017-14283-2, 2017.

Szalai, S. and Szinell, C.: Comparison of two drought indices for drought monitoring in Hungary – a case study, in: Drought and Drought Mitigation in Europe, edited by: Somma, F. and Vogt, J. V., Springer, Berlin, 161–166, 2000.

Tannehill, I. R.: Drought: its causes and effects, Princeton Univ. Press, Princeton, N.J., 1947.

Ting, M., Seager, R., Li, C., Liu, H., and Henderson, N.: Mechanism of Future Spring Drying in the Southwestern United States in CMIP5 Models, J. Climate, 31, 4265–4279, https://doi.org/10.1175/JCLI-D-17-0574.1, 2018.

Vanderlinden, K.: Análisis de procesos hidrológicos a diferentes escalas espacio-temporales, PhD Diss., University of Córdoba, Dept. of Agronomy, Córdoba, Spain, 2001 (in Spanish).

Van Loon, A. F. and Van Lanen, H. A. J.: A process-based typology of hydrological drought, Hydrol. Earth Syst. Sci., 16, 1915–1946, https://doi.org/10.5194/hess-16-1915-2012, 2012.

Van Loon, A. F. and Laaha, G.: Hydrological drought severity explained by climate and catchment characteristics, J. Hydrol., 526, 3–14, 2015.

Wang, L. and Yuan, X.: Two types of flash drought and their connections with seasonal drought, Adv. Atmos. Sci., 35, 1478–1490, 2018.

Wilhite, D. A. and Glantz, M. H. Understanding the drought phenomenon: the role of definitions, Water Int., 10, 111–120, 1985.

Wilhite, D. A., Hayes, M. J., Kinutson, C., and Smith, K. H.: Planning for drought: moving from crisis to risk management, J. Am. Water Resour. As., 36, 697–710, 2000.

Yang, T., Ding, J., Liu, D., Wang, X., and Wang, T.: Combined use of multiple drought indices for global assessment of dry gets

drier and wet gets wetter paradigm, J. Climate, 32, 737–748, 2019.

Zarch, M. A. A., Sivakumar, B., and Sharma, A.: Droughts in a warming climate: A global assessment of Standardized precipitation index (SPI) and Reconnaisance drought index (RDI), J. Hydrol., 526, 183–195, 2015.

Chapter 3

Impact of Climate Change on Agricultural Droughts in Spain

water

MDPI

Article

Impact of Climate Change on Agricultural Droughts in Spain

María del Pilar Jiménez-Donaire [1,*], Juan Vicente Giráldez [1,2] and Tom Vanwalleghem [1]

[1] Department of Agronomy, University of Córdoba, 14071 Córdoba, Spain; ag1gicej@uco.es (J.V.G.); ag2vavat@uco.es (T.V.)
[2] Institute for Sustainable Agriculture, CSIC, 14071 Córdoba, Spain
* Correspondence: g52jidom@uco.es

Received: 22 October 2020; Accepted: 12 November 2020; Published: 17 November 2020

Abstract: Drought is an important natural hazard that is expected to increase in frequency and intensity as a consequence of climate change. This study aimed to evaluate the impact of future changes in the temperature and precipitation regime of Spain on agricultural droughts, using novel static and dynamic drought indices. Statistically downscaled climate change scenarios from the model HadGEM2-CC, under the scenario representative concentration pathway 8.5 (RCP8.5), were used at a total of 374 sites for the period 2006 to 2100. The evolution of static and dynamic drought stress indices over time show clearly how drought frequency, duration and intensity increase over time. Values of static and dynamic drought indices increase over time, with more frequent occurrences of maximum index values equal to 1, especially towards the end of the century (2071–2100). Spatially, the increase occurs over almost the entire area, except in the more humid northern Spain, and in areas that are already dry at present, which are located in southeast Spain and in the Ebro valley. This study confirms the potential of static and dynamic indices for monitoring and prediction of drought stress.

Keywords: climate change; drought stress; drought monitoring; plant water stress; Spain

1. Introduction

Climate change is one of the greatest future challenges for society as a whole, and for agricultural production and food security specifically [1]. If the current situation of greenhouse gas emissions continues, agricultural productivity will be significantly affected, with temperature increases and rainfall decreases offsetting benefits of increased carbon dioxide concentrations [2]. Arora [3] reports an estimated 20–45% decline in maize (*Z. mays*) yields, 5–50% in wheat (*Triticum* L.) and 20–30% in rice (*Oryza sativa*). In Europe, a series of research projects of the Joint Research Centre, called PESETA, have analyzed in more detail the climate change impacts on a wide range of environmental and socio-economic aspects [4], showing clearly very uneven impacts within the EU and an important north-south divide. Southern Europe is hit especially hard, with a significant decline in agricultural production, whereas some parts of eastern and northern Europe show production increases. However, this type of assessment of crop yield under climate change is entirely based on crop-growth models, which often do not allow to take into account climate extremes, such as drought or freezing events. Trnka et al. [5] evaluated future agroclimatic conditions in Europe and found worsening conditions in most of Europe, including eastern and northern Europe. They attribute this to a higher risk of extremely unfavorable years that are likely to increase everywhere, for example, due to for example drought stress, frost, or the absence of snow cover that does not protect against frost.

It is well known that extreme events, such as heat waves and droughts, are projected to increase over the next decades [1]. Lu et al. [6] evaluated the uncertainty related to agricultural drought predictions from the Coupled Model Intercomparison Project phase 5 (CMIP5) models at a global

scale. They identified Europe and the Mediterranean as being among the hotspots, where droughts are expected to increase most notably for all analyzed emission scenarios. Pausas and Millan [7] indicate that in the Mediterranean the situation might be more complex because, due to socio-economic feedback loops, land abandonment of less suitable agricultural areas might actually lead to vegetation recovery, or greening, as opposed to the drying or browning process caused by human-induced climate change.

Different studies have addressed the increase of droughts in Europe and in the Mediterranean region under projected climate change scenarios. In order to correctly assess the impact of future climate change on agricultural droughts, it is crucial to use adequate drought indicators and work at the finest spatial scale possible. Firstly, drought indicators need to take into account both the decrease in rainfall, as well as the increase in temperature and evapotranspiration. Especially for agricultural purposes, it is crucial to have a correct representation of buffering soil moisture dynamics. Many studies, for example, have assessed the occurrence of meteorological droughts under future climate change, using the Standardized Precipitation Index (SPI), which only accounts for changes in the rainfall regime. Secondly, climate change projections are normally based on simulations from general circulation models (GCMs) that are run under various emission scenarios. The results however cannot be directly applied to climate change impact studies, and further downscaling is needed [8]. Higher resolution can be obtained by regional climate models (RCMs), nested within a GCM, but these generally inherit the biases and other deficiencies of the large-scale model and further, statistical, downscaling is needed. The basic idea behind statistical downscaling is to define a relationship between the large-scale model (either GCM or RCM) and the local climate [8].

Several studies analyze meteorological drought by means of RCMs. For instance, Maule et al. [9] used the SPI and a version of the Palmer drought severity index (PDSI) to analyze drought representation by 14 RCMs from the ENSEMBLES project [10] at a European scale. They conclude that, at a European scale, the results seem robust but warn to use quantitative results at smaller, regional scales. RCMs are also used frequently in soil moisture and hydrological drought analyses. Spinoni et al. [11] used climate predictions from the EURO-CORDEX to evaluate drought events at a European scale, by means of standardized precipitation index (SPI), standardized precipitation evapotranspiration index (SPEI) and the reconnaissance drought indicator (RDI). More detailed studies were carried out in different countries, using the data from the EURO-CORDEX project. For example, Meresa et al. [12] studied hydro-meteorological drought in ten Polish catchments by computing SPI, the Standardized Precipitation Evapotranspiration Index (SPEI) and runoff standardized indices for 1971–2100. They concluded that SPI and SRI indicated wetter conditions in the future, while SPEI indicated a drying trend. Potopová et al. [13] also used results from eight RCMs from the EURO-CORDEX project to calculate future drought trends in the Czech Republic, by means SPI and SPEI. Barrella-Ortiz and Quintana-Seguí [14] evaluated drought representation and propagation in three RCMs from the Med-CORDEX database, focusing on the Mediterranean region. They conclude that RCMs are a suitable tool for meteorological drought studies, but that they should be used cautiously for soil moisture and hydrological drought analyses.

Drought studies using statistically downscaled climate projections are much rarer, and have not been done for Spain, according to the knowledge of the authors. In addition, recent studies have shown that for drought prediction and monitoring it is crucial to take into account the buffering effect that soil properties have, as well as crop type and cropping characteristics. Jiménez-Donaire et al. [15] recently analyzed the potential of two new indicators, static and dynamic drought stresses, based on earlier work by Porporato et al. [16]. In a study under cereal in Southern Spain, they concluded both indicators identified agricultural droughts well and were found to be good predictors of crop yield.

The objective of this study is to analyze the effect of climate change on agricultural drought in Spain, using these novel static and dynamic drought stress indicators and statistically downscaled climate change predictions for the period 2006 to 2100.

2. Materials and Methods

2.1. Study Area

This study was conducted throughout mainland Spain and the Balearic Islands. The time period was limited to 2006–2100, because of the availability of statistically downscaled regional climate model (RCMs) projections.

Spain can be subdivided in three main biogeographical regions (Figure 1). Most of the country is classified as Mediterranean, with the exception of the northern coastal region that is Atlantic and the Pyrenees mountain range, which is classified as Alpine [17]. The Mediterranean biogeographical region corresponds to a temperate climate region (type C), according to the Köppen classification system, and can be further subdivided into hot and warm summer Mediterrean Climate, Csa and Csb, respectively, which are considered typically Mediterranean climate zones, and cool-summer Mediterranean climate, Csc. Some parts of this biogeographical region of Spain are also drier and are also classified as dry climates (type B, specifically hot deserts climate, BWh, cold desert climate, BWk, and hot semi-arid climate, BSh). These are located in the southeast coastal regions of Murcia, Almeria and Valencia and the Ebro valley. The northern Atlantic biogeographical region mostly corresponds to temperate climate (type C) without a dry summer (humid subtropical and oceanic climate, Cfa and Cfb). The Alpine regions correspond to cold climate types without dry season (warm summer continental and subarctic climate, Dfb and Dfc).

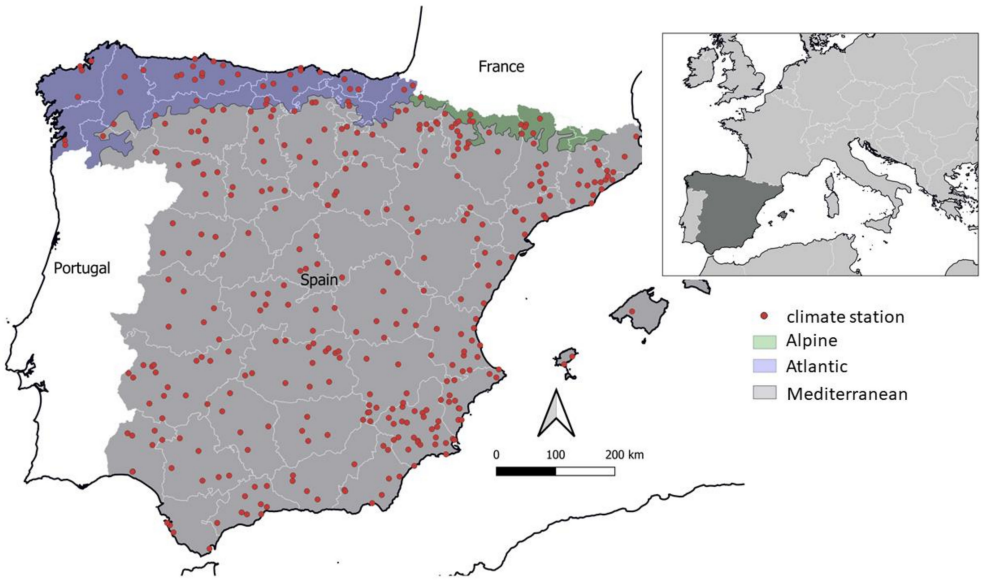

Figure 1. Biogeographical regions and location of used climate stations within Spain. Inset shows Spain within Europe. White lines indicate province boundaries.

2.2. Climate Change Data

In this study, statistically regionalized projections of climate change are used that were developed by the Spanish National Agency for Meteorology. Daily precipitation, maximum and minimum temperature data between 2006 and 2100 were used from the model HadGEM2-CC, under the scenario RCP8.5, from the Intergovernmental Panel on Climate Change's fifth assessment report. These data are available for free download [18]. This study only evaluates this emission scenario, as no statistically downscaled data for Spain were available at present for this model under other scenarios, such as, for example RCP4.5, which is another frequently used scenario that establishes a more moderate greenhouse gas increase. The scenario RCP8.5 used here assumes that emissions continue to rise at the present level throughout the 21st century. This scenario is generally taken as the basis for the worst-case climate change scenario and, while it has received some criticism by some reports

because it is considered implausible, it is useful, as it allows tracking and predicting the effect of our current behavior, and makes it possible to demonstrate the impact of emission reduction policies if no action were to be taken. In addition, some recent research has concluded that this scenario with a high temperature increase at the end of this century is becoming increasingly more plausible because of feedback effects [19–21]. In total, daily data between 2006–2100 was available for 374 stations. The distribution of these stations is shown in Figure 1.

Calculations of soil water balance and drought stress indicators were made for each of these points in R 4.0.0 [22] with packages dplyr, tidyverse and yarrr. Output maps were generated in QGIS 3.10.6 [23].

2.3. Drought Stress Indicators: Static and Dynamic Stress

A full description of the calculation of the static and dynamic stress drought indicators is given in Jiménez-Donaire et al. [15]. Static stress (ζ) is proportional to the excursion of soil moisture (W) below a critical point that corresponds to incipient stomatal closure (W^*), and reaches a maximum equal to 1 for soil moisture values below permanent wilting point (W_{pwp}). It is calculated as:

$$\begin{cases} \zeta(t) = 0, \text{ for } W(t) > W^* \\ \zeta(t) = 1, \text{ for } W(t) < W_{pwp} \\ \zeta(t) = \left[\frac{W^* - W(t)}{W^* - W_{pwp}}\right]^q, \text{ for } W_{pwp} \le W(t) \le W^* \end{cases} \quad (1)$$

Plant stress can increase non-linearly with soil moisture deficit, where the coefficient q is a measure of this non-linearity. In this study a value of 1 was used, implying a linear soil moisture-stress relation. The static stress $\zeta(t)$ is calculated at daily time steps, and the overall static water stress, ζ, is then calculated by integrating the individual positive values of $\zeta(t)$ over the whole year, excluding periods where $\zeta(t) = 0$.

Dynamic stress (θ) includes information on the mean duration and frequency of drought periods. This indicator therefore extends the information contained in the static stress indicator, as the latter only takes into account the intensity of the droughts that occur over a year. The expression for θ is:

$$\begin{cases} \theta = \left(\frac{\zeta\, T_{W^*}}{k\, T_{seas}}\right)^{1/\sqrt{n_{W^*}}}, \text{ if } \zeta\, T_{W^*} < k\, T_{seas} \\ \theta = 1, \textit{ otherwise} \end{cases} \quad (2)$$

where n_{W^*} and T_{W^*} are the number (-) and mean duration (days) of all drought occurrences over a year, respectively, T_{seas} is the duration of the growing season (days) and k is a parameter, set to 0.5 following Porporato et al. [16].

The soil water balance is calculated using the same approach as Jiménez-Donaire et al. [15], using a simple bucket model applied over the root zone, and taking into account the main processes of rainfall infiltration (f), evapotranspiration (e) and deep seepage (g). The calculated soil moisture values $W(t)$, are representative of the mean moisture content over the root zone depth, taken as 1m.

$$\frac{dW(t)}{dt} = f - e - g \quad (3)$$

The main difference with the previous study the future climate change prediction datasets are lacking detailed information on meteorological variables needed to calculate reference evapotranspiration using FAO Penman-Monteith's formula. Therefore, Hargreaves' formula [24,25] was used to calculate reference evapotranspiration from the minimum and maximum temperature data:

$$e_0 = AHC\, R_a (T + 17.8) \sqrt{(T_{max} - T_{\min})} \quad (4)$$

where R_a is the water equivalent of extraterrestrial radiation (mm day^{-1}); T, T_{max} and T_{min} are the daily mean, maximum and minimum temperatures (C), respectively; AHC is the adjusted Hargreaves coefficient, equal to 0.0023 in the original equation. Although some studies have pointed to regional differences and have proposed locally calibrated values [26], this value was used for the entire study area as it is sufficiently robust [25] and no estimates are available for the different parts of Spain. Finally, the real daily evapotranspiration rate is calculated by correcting this potential rate, e_0, by the wetness of the soil profile, ω, and the crop coefficient, k_c:

$$e = \omega k_c e_0 \quad (5)$$

Static and dynamic drought stress indicators were calculated for the period 2006–2100, and their evolution was analyzed over 3 time periods: 2006–2040, 2041–2070 and 2071–2100.

3. Results

3.1. Spatial and Temporal Trends in Static and Dynamic Drought Stress between 2006–2100

The behavior of two representative sites, respectively for the southern, semi-arid part of Spain, and for the northern, more humid part of Spain, is analyzed first to illustrate behavior of the drought indices and their evolution over the study period. Most of mainland Spain is characterized by relatively dry Mediterranean climate, with a clear dry season. Drought incidence is already a frequent phenomenon, as the observed year-to-year rainfall variability is relatively high. This means that years where rainfall falls below 500 mm are already frequent at present. This behavior reflects in the climate projections for the period 2006–2100 shown in Figure 2a, for the La Rambla site, Córdoba province, which can be taken as a representative site of this climate zone. The coefficient of variation of the annual precipitation is 31%. At the same time, the climate projections indicate a significant decrease in precipitation that amounts to 0.45% per year, translating in a decrease of the mean annual precipitation of 530 mm between 2006–2040 to 498 mm for 20341–2070, and decreasing even more strongly to 399 mm for 2071–2100. This is clearly reflected in the static and dynamic drought stress indices. While this semiarid zone has already an incidence of important drought events at the beginning of the study period, the occurrence of serious drought events, with values of static and dynamic stress hitting highs equal to the maximum value of 1, increases strongly by 2071–2100. The mean static stress increases from 0.49 in 2006–2040, to 0.57 in 2041–2070 and 0.76 in 2071–2100. Over the same periods, the dynamic stress increases from 0.35, to 0.44 and 0.69, respectively. The occurrences of dynamic stress values equal to 1, implying that soil moisture remains below the critical soil moisture level during the entire growing season, and increases from 2 to 4 to 18 times in the three different periods (2006–2040, 2041–2070 and 2071–2100).

In contrast, the stress indices in the northern Spanish site of Lugo, province of Lugo, shown in Figure 2b, are much lower due to a higher rainfall regime and the absence of a dry season. Even so, precipitation decreases significantly at a rate of 0.28% year^{-1}. Mean annual precipitation lowers from 997 mm between 2006–2040, to 952 mm between 2041–2070 to 831 mm for the last period 2071–2100. Overall drought stress levels are low, generally lower than the minimum values that are reached at the La Rambla site, so no crop stress should be expected. However, also at this site an increase can be observed over the studied period due to climate change, especially for the last period. The mean static stress index remains at 0.07 between 2006–2040 and 2041–2070, but rises to 0.18 for 2071–2100. The same behavior is seen for dynamic stress, almost stable at 0.03 and 0.04 between 2006–2040 and 2041–2070, respectively, and increasing to 0.12 for 2071–2100. However, static and dynamic stress never reaches 1, even in the years with minimum annual precipitation of the series.

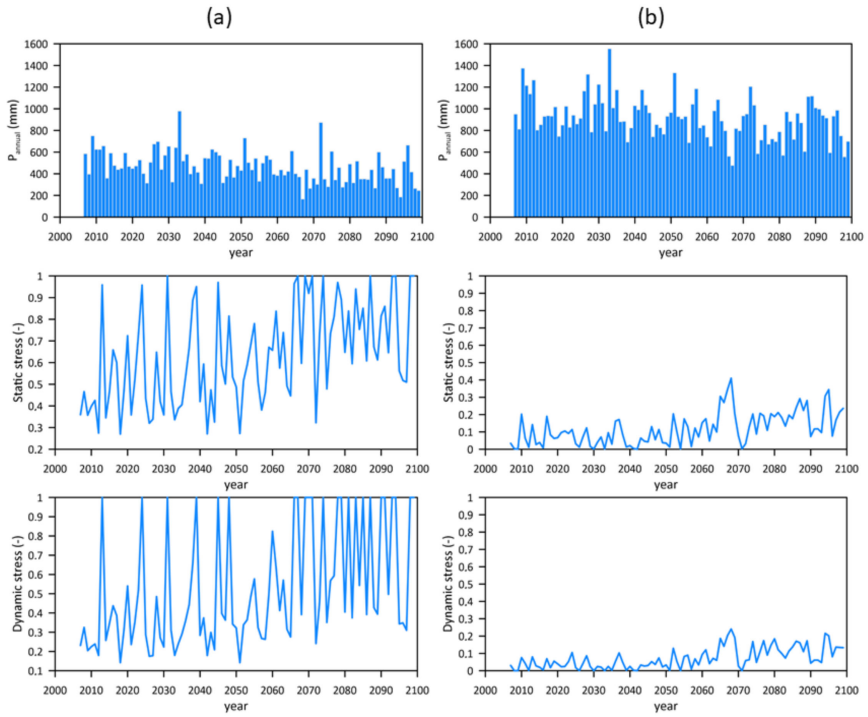

Figure 2. Evolution of precipitation, static stress and dynamic stress between 2006–2100, for a site in southern Spain and northern Spain, respectively: (**a**) site La Rambla, Córdoba (N 37.606, W −4.741); (**b**) Lugo, Lugo (N 43.011, W −7.555).

Spatial trends of static and dynamic stress for the periods 2006–2100 are shown in Figures 3 and 4. Static and dynamic stresses are classified in 5 levels: no stress, very low (0–0.2), low (0.25–0.50), moderate (0.50–0.75) and high stress (0.75–1.00). In the first period of 2006–2040, high levels of static and dynamic stress (0.75–1.00) are observed in the southeast of Spain and the Ebro valley, which are already characterized by a dry climate. The northern Atlantic region, with more abundant precipitation is characterized by no stress (no data) to very low stress values (0–0.25). Most of mainland Spain is characterized by low to moderate levels (0.25–0.50 and 0.50–0.75). Over the years, especially during the last period 2071–2100 it can be observed how most of mainland Spain evolves to increasing drought stress and more sites are characterized by high static and dynamic stress levels, over 0.75.

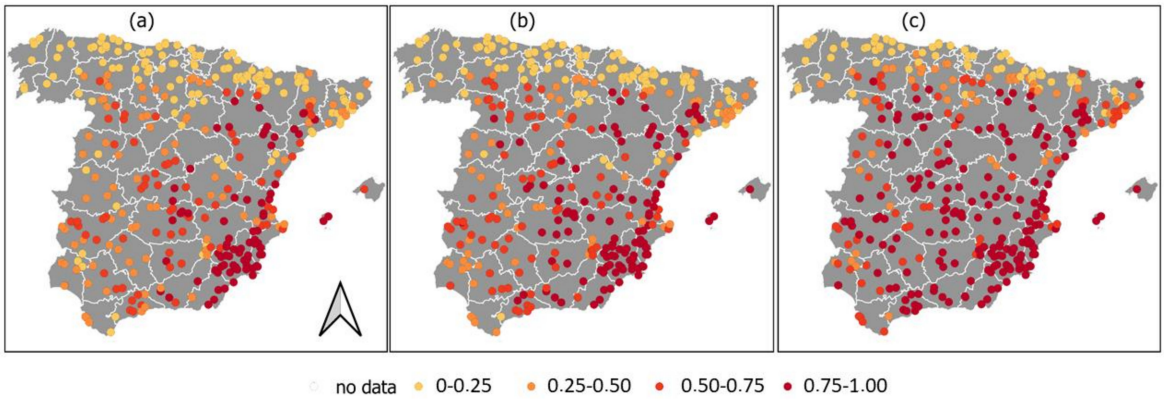

Figure 3. Average value of the static stress indicator in Spain over the periods 2006–2040 (**a**); 2041–2070 (**b**); and 2071–2100 (**c**).

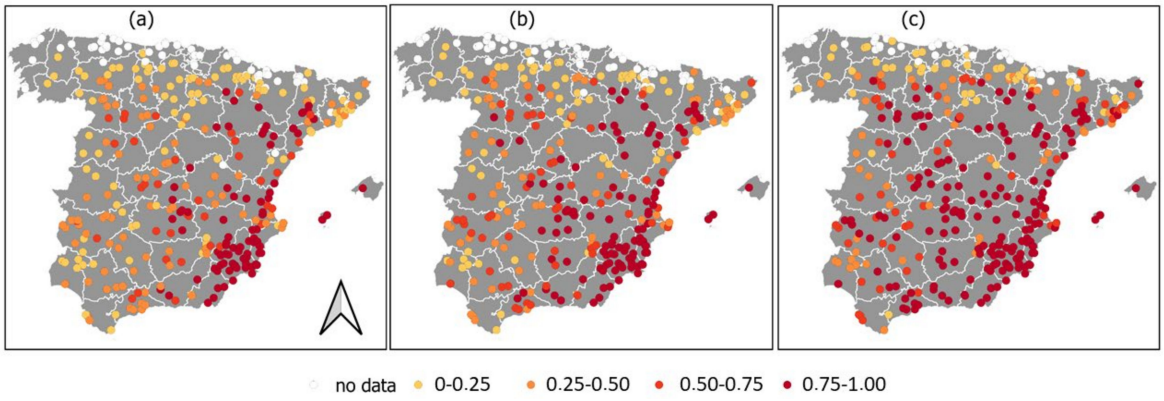

Figure 4. Average value of the dynamic stress indicator in Spain over the periods 2006–2040 (**a**); 2041–2070 (**b**); and 2071–2100 (**c**).

Figure 5 summarizes the temporal changes in static and dynamic drought stress, comparing the period 2006–2040 versus 2041–2070 (a and c), and 2006–2040 versus 2071–2100 (b and d). Both drought stress indicators show the same trends. Firstly, the sites in areas that are already dry, and characterized by high stress levels that, at present, show almost no change over time, or even a small decrease in mean drought stress, showing up in blue. These points are located along the southeastern Spain and in the Ebro valley. However, the rest of Spain shows a significant change with respect to the reference period 2006–2040. Change is moderate for the second period, 2041–2071, for most sites with increases contained below 30%. However, especially for the last periods, most sites show up in dark red, indicating changes of over 45%. For sites that start out with low absolute drought stress values, such as those in the north of Spain, this does not imply important problems with crop production, although some sites change from no stress condition to low stress condition. However, for most of mainland Spain, already characterized by moderate to high stress levels in 2006–2040, this increase indicates an alarming situation and flags problems with droughts affecting agricultural crop production in most of the country.

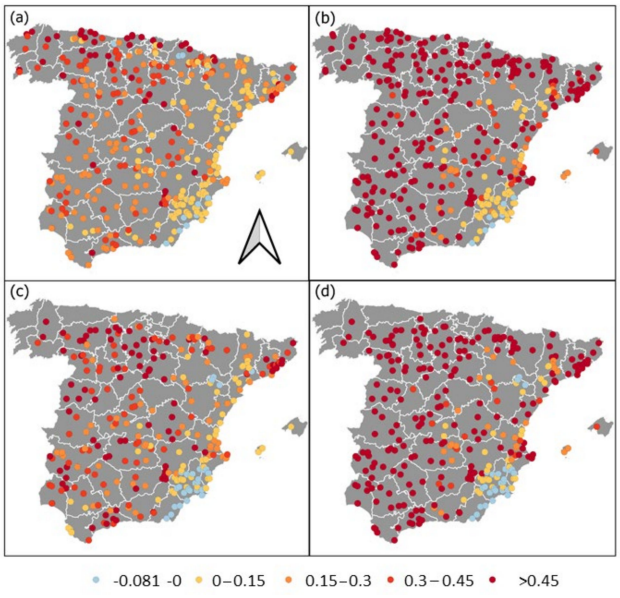

Figure 5. Increase of the static drought stress in Spain over the periods: (**a**) 2006–2040 vs. 2041–2070 and (**b**) 2006–2040 vs. and 2071–2100; and increase of the dynamic drought stress over the periods (**c**) 2006–2040 vs. 2041–2070 and (**d**) 2006–2040 vs. 2071–2100. Change is indicated as fractional and negative values indicate a drought stress decrease.

3.2. Analysis of Static and Dynamic Stress Index Dynamics

The relation between annual precipitation and static and dynamic stress is shown in Figure 6. It can be seen that the relation of both indicators with rainfall is highly non-linear and increases sharply below approximately 500 to 600 mm annual rainfall. Where rainfall is higher, it is very rare to have droughts. However, within this range of annual rainfall, the variation of static and dynamic stress indices is high, and can range from 0 (no stress) to 1 (maximum stress), depending on how the precipitation is distributed throughout the growing season. This illustrates clearly how rainfall alone is not a good indicator of agricultural drought stress.

The relation between static and dynamic stress is shown in Figure 7. It can be seen how most points are clustered, except for a few points that are limited by the maximum envelope, as, for static stress values higher than 0.8, dynamic stress reaches the maximum of 1.

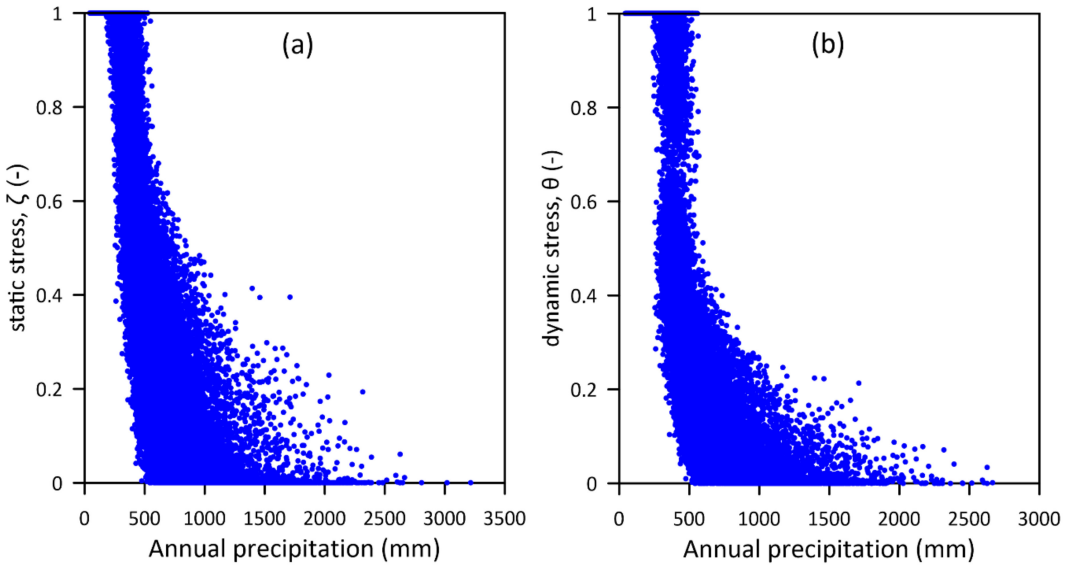

Figure 6. Relation between annual precipitation and (**a**) dynamic and (**b**) static stress for all sites and studied years

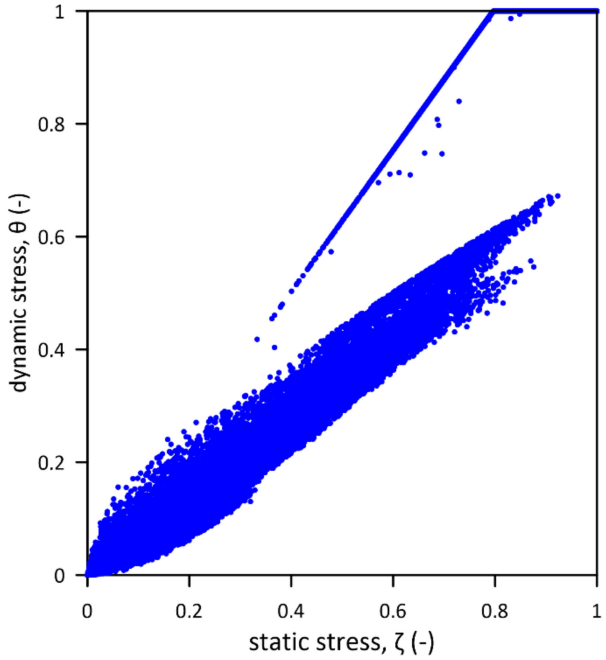

Figure 7. Relation between dynamic and static stress for all sites and studied years.

4. Discussion

In Spain and in the Mediterranean basin specifically, agriculture has always been affected by large natural climate variability and by droughts. Historically, Spain has suffered important droughts. Domínguez-Castro [27] analyzed Spanish drought episodes over the past 500 years, based on ceremonial records and tree rings. They reported frequent droughts since the start of their historical records in the 16th century, with the most severe droughts being recorded during the period from the end of the 16th century up until the 18th century. Additionally, in recent times, Spain has suffered several intense drought episodes [28], and some of the most notorious ones in terms of impact were produced during the periods: 1941–1945, 1979–1983, 1991–1995 and 2004–2007 [29]. Jiménez-Donaire et al. [30] studied drought incidence in the south of Spain between 2003 and 2013, and reported two severe drought periods (2004–2005 and 2011–2012) with associated crop damages between 70 and 95% of the agriculturally insured area. The concern of Spain with droughts is reflected by the presence of drought response measures and planning in policy tools, such as the National Hydrologic Plan Act [31].

This study demonstrates that the novel indicators static and dynamic drought stress, proposed by Jiménez-Donaire et al. [15], are useful for analyzing drought dynamics at regional level. The results, using statistically downscaled climate projections at regional level, indicate that if greenhouse gas emissions continue at the present level, drought occurrence will increase significantly between 2041–2070, and especially between 2071–2100, compared to the reference period of 2006–2040. In the Mediterranean areas, severe droughts with maximum values of static and dynamic droughts equal to 1 are shown to increase in magnitude, duration and frequency. Drought incidence increases over the whole country, except in the north and southeast. In northern, more humid regions, static and dynamic drought indices are below 0.25, and not limiting for crop growth, although they also experience an increase towards the end of the studied period. In the southeast and part of the Ebro valley, drought occurrence is already very high in the reference period 2006–2040.

Similar results were obtained by Spinoni et al. [32] using SPI and SPEI indices at European level. They considered three periods, 1981–2010, 2041–2070 and 2071–2100. For this last period, their results indicated more frequent and severe extreme droughts over the whole European continent, except Iceland, under the most severe emission scenario (RCP8.5) that was used here. They reported especially severe increases in southern Europe. For the Iberian Peninsula, a strong increase, meaning an increase of more than one additional event every 10 years, in more than 80% of the area for all seasons except winter, where a more moderate increase was observed. Our results are specifically designed to consider specifically the growing season only, with precipitation during fall, winter and spring being particularly important, whereas an increase of droughts during the summer dry period can be expected to have little or no effect on the evolution of soil moisture during the growing season, and therefore will also have little effect on static and dynamic drought indices. Marcos-Garcia et al. [33] studied climate change impact on meteorological drought and hydrological drought in the Mediterranean basin of the Jucar river. Although their predictions are geared towards the smaller river basin scale and at the mid-term (i.e., up to 2069), their results also show a similar trend using a normalized SPI and SPEI. They report a future decrease in the number of dry spells for the RCP8.5 scenario, but an increase of the average duration and intensity, meaning that often a single dry spell covers the entire analysis period instead of several, shorter dry spells. They also conclude that temperature effects on increase of evapotranspiration should not be ignored, and therefore SPEI is more useful than SPI. In our study, this effect was taken into account by resolving the full soil moisture balance over the period 2006–2100 for all studied sites. Gaitán et al. [34] studied future droughts in the Aragon region in northeast Spain, covering part of the Ebro valley, for two RCPs, RCP4.5 and 8.5. Their results, also based on the use of the SPI and SPEI indices, confirm the clear trend toward increasingly intense periods of droughts, especially towards the end of century for the period 2071–2100. Interestingly, they report this is only detected when considering SPEI, which in addition to precipitation takes into account evapotranspiration, but is softened in the SPI scenarios. At the spatial scale, they also observed the most affected region to be the Ebro valley.

Global change has been reported to lead to drought increase in several regions around the globe, In some areas, it is caused by a combination of temperature increase and precipitation decrease, as this study has shown for the case of Spain, while in other regions droughts increase, in spite of precipitation increase, due to the dominating effect of temperature increase. Wang et al. [35] studied the increase of drought frequency and characteristics in the Huai river basin in China. They used the SPEI index and found that although climate change models project an increase in precipitation, it was not enough to offset the increased evapotranspiration due to temperature increases. Similar to this study, they reported a slight increase in droughts at the beginning of the 21st century, and a strong increase towards the end of the 21st century. In other areas droughts might increase due to even more complex situations. In Poland in central Europe, Sojka et al. [36] report an increase in the extension of rain-free periods, in spite of an overall precipitation increase. Their study shows that this results in a decrease of mean groundwater levels, and a reduction of subsurface flow. They report in contrast an increase of extreme events, leading to more runoff, but this water cannot be stored in the soil and used for agricultural crop production. Amnuaylojaroen and Chanvichit [37] analyzed the tendency of agricultural drought under climate change for Mainland Southeast Asia, using the SPI and crop water need (CWN) indices. The compared present-day with the period 2020–2029 under the scenario RCP8.5. Again, their climate predictions favor drought increase for this region, due to the combination of precipitation decrease and temperature increase. However, they only reported a change in SPI, while their index CWN, which would, in theory, be better suited, as it takes into account evapotranspiration, did not indicate drought increase.

This study aimed to characterize drought patterns across Spain under the worst-case emission scenario RCP8.5. The use of RCP8.5 impacts our results, as it the high end of CO_2 emissions and temperature increase. While different authors consider such high temperature increases more and more likely, as discussed earlier [19–21], it would be useful to examine other, more conservative scenarios in future studies. Follow-up studies should also explore different climate models from the CMIP5 ensemble. In any case, our results show that static and dynamic drought stress indicators are very useful to evaluate drought stress under climate change. Static drought stress indicates the drought magnitude, and dynamic drought stress incorporates additional information on duration and frequency of these drought events. This latter indicator therefore allows to obtain information on different aspects of drought (magnitude, duration and frequency) with a single indicator.

5. Conclusions

The objective of this study was to evaluate the suitability of static and dynamic stress as indicators of agricultural drought stress, and to use these indicators to evaluate spatial and temporal patterns of agricultural drought stress under climate change in Spain. The results show that static and dynamic drought stress are highly suitable indicators. Static drought stress indicates the magnitude of drought stress, while dynamic drought stress also includes frequency and duration of drought events. Both are shown to increase in the 21st century, especially towards the end of the studied period. Changes are significant for most of mainland Spain, which is under a Mediterranean climate. Only in the southeastern areas that are already very dry and in the northern areas that are humid, is the impact of climate change on droughts absent to low.

The projected climate scenarios and the methodology used in this study have several limitations. For example, it is expected that, for crops and pastures, production will be delayed by the onset of autumn rainfall. Water scarcity and other climate-induced changes to the cropping cycle, such as for example phenological changes or chilling requirements, might also change the suitability of entire regions for certain crops altogether and force shifting cropping patterns. Such changes in the growing season would be very interesting to address in future studies. To include these adaptations of crop production, it is necessary to couple crop simulation models with socio-economic modelling. Such efforts are underway in the framework of large international modelling efforts, such as AgMIP8 [38] or MACSUR [39], but need to take into account extreme events such as the droughts modelled here.

Author Contributions: Conceptualization, T.V.; methodology, M.d.P.J.-D.; software, M.d.P.J.-D. and T.V.; formal analysis, M.d.P.J.-D.; investigation, M.d.P.J.-D. and T.V.; writing—original draft preparation, M.d.P.J.-D.; writing—review and editing, M.d.P.J.-D., J.V.G. and T.V.; visualization, M.d.P.J.-D. and T.V.; supervision, J.V.G. and T.V.; project administration, T.V.; funding acquisition, T.V. All authors have read and agreed to the published version of the manuscript.

Funding: This study was funded by the research projects AGL2015-65036-C3-2-R and PID2019-109924RB-I00 financed by the "Programas estatales de generación de conocimiento y fortalecimiento científico y tecnológico del sistema de I + D + i y de I + D + I orientada a los retos de la sociedad".

Acknowledgments: The climate data projections were obtained from the Climatic Services of the Spanish National Agency for Meteorology (Agencia Estatal de Meteorología), Ministry of Ecological Transition and Demographic Challenges (MITECO).

Conflicts of Interest: The authors declare no conflict of interest.

References

1. Schmidhuber, J.; Tubiello, F.N. Global food security under climate change. *Proc. Natl. Acad. Sci. USA* **2007**, *104*, 19703–19708. [CrossRef] [PubMed]
2. Gornall, J.; Betts, R.; Burke, E.; Clark, R.; Camp, J.; Willett, K.; Wiltshire, A. Implications of climate change for agricultural productivity in the early twenty-first century. *Philos. Trans. R. Soc. B Biol. Sci.* **2010**, *365*, 2973–2989. [CrossRef] [PubMed]
3. Arora, N.K. Impact of climate change on agriculture production and its sustainable solutions. *Environ. Sustain.* **2019**, *2*, 95–96. [CrossRef]
4. Ciscar Martinez, J.C.; Ruiz, D.; Ramirez, A.; Dosio, A.; Toreti, A.; Ceglar, A.; Fumagalli, D.; Dentener, F.; Lecerf, R.; Zucchini, A.; et al. *Climate Impacts in Europe: Final Report of the JRC PESETA III Project*; European Commission: Luxembourg, 2018.
5. Trnka, M.; Olesen, J.E.; Kersebaum, K.C.; Skjelvåg, A.O.; Eitzinger, J.; Seguin, B.; Peltonen-Sainio, P.; Rötter, R.; Iglesias, A.; Orlandini, S.; et al. Agroclimatic conditions in Europe under climate change. *Glob. Chang. Biol.* **2011**, *17*, 2298–2318. [CrossRef]
6. Lu, J.; Carbone, G.J.; Grego, J.M. Uncertainty and hotspots in 21st century projections of agricultural drought from CMIP5 models. *Sci. Rep.* **2019**, *9*, 4922. [CrossRef]
7. Pausas, J.G.; Millán, M.M. Greening and Browning in a Climate Change Hotspot: The Mediterranean Basin. *BioScience* **2019**, *69*, 143–151. [CrossRef]
8. Sunyer, M.A.; Madsen, H.; Ang, P.H. A comparison of different regional climate models and statistical downscaling methods for extreme rainfall estimation under climate change. *Atmos. Res.* **2012**, *103*, 119–128. [CrossRef]
9. Maule, C.F.; Thejll, P.; Christensen, J.H.; Svendsen, S.H.; Hannaford, J. Improved confidence in regional climate model simulations of precipitation evaluated using drought statistics from the ENSEMBLES models. *Clim. Dyn.* **2013**, *40*, 155–173. [CrossRef]
10. Van der Linden, P.; Mitchell, J.F.B. *ENSEMBLES: Climate Change and its Impacts. Summary of Research and Results from the ENSEMBLES Project*; Met Office Hadley Centre: Devon, UK, 2009.
11. Spinoni, J.; Barbosa, P.; Bucchignani, E.; Cassano, J.; Cavazos, T.; Christensen, J.H.; Christensen, O.B.; Coppola, E.; Evans, J.; Geyer, B.; et al. Future Global Meteorological Drought Hot Spots: A Study Based on CORDEX Data. *J. Clim.* **2020**, *33*, 3635–3661. [CrossRef]
12. Meresa, H.K.; Osuch, M.; Romanowicz, R. Hydro-Meteorological Drought Projections into the 21-st Century for Selected Polish Catchments. *Water* **2016**, *8*, 206. [CrossRef]
13. Potopová, V.; Štěpánek, P.; Zahradníček, P.; Farda, A.; Türkott, L.; Soukup, J. Projected changes in the evolution of drought on various timescales over the Czech Republic according to Euro-CORDEX models. *Int. J. Climatol.* **2018**, *38*, e939–e954. [CrossRef]
14. Barella-Ortiz, A.; Quintana-Seguí, P. Evaluation of drought representation and propagation in regional climate model simulations across Spain. *Hydrol. Earth Syst. Sci.* **2019**, *23*, 5111–5131. [CrossRef]
15. Jiménez-Donaire, M.d.P.; Giráldez, J.V.; Vanwalleghem, T. Evaluation of Drought Stress in Cereal through Probabilistic Modelling of Soil Moisture Dynamics. *Water* **2020**, *12*, 2592. [CrossRef]

16. Porporato, A.; Laio, F.; Ridolfi, L.; Rodriguez-Iturbe, I. Plants in water-controlled ecosystems: Active role in hydrologic processes and response to water stress: III. Vegetation water stress. *Adv. Water Resour.* **2001**, *24*, 725–744. [CrossRef]
17. European Environment Agency. Biogeographical Regions in Europe. Available online: https://www.eea.europa.eu/data-and-maps/figures/biogeographical-regions-in-europe-2 (accessed on 20 October 2020).
18. AEMET. Proyecciones Climáticas para el siglo XXI-Datos Diarios. Available online: http://www.aemet.es/es/serviciosclimaticos/cambio_climat/datos_diarios?w=0&w2=0&cm=analogos&mo=MPI-ESM-LR&es=Todos&va=Todos&pe=2006-2100&b=1 (accessed on 27 August 2020).
19. Friedlingstein, P.; Meinshausen, M.; Arora, V.K.; Jones, C.D.; Anav, A.; Liddicoat, S.K.; Knutti, R. Uncertainties in CMIP5 Climate Projections due to Carbon Cycle Feedbacks. *J. Clim.* **2014**, *27*, 511–526. [CrossRef]
20. Lenton, T.M.; Rockström, J.; Gaffney, O.; Rahmstorf, S.; Richardson, K.; Steffen, W.; Schellnhuber, H.J. Climate tipping points—Too risky to bet against. *Nature* **2019**, *575*, 592–595. [CrossRef]
21. Peters, G.P.; Andrew, R.M.; Boden, T.; Canadell, J.G.; Ciais, P.; Le Quéré, C.; Marland, G.; Raupach, M.R.; Wilson, C. The challenge to keep global warming below 2 °C. *Nat. Clim. Chang.* **2013**, *3*, 4–6. [CrossRef]
22. R Core Team. *R: A Language and Environment for Statistical Computing*; R Foundation for Statistical Computing: Vienna, Austria, 2020.
23. QGIS Development Team. QGIS Geographic Information System. Open Source Geospatial Foundation Project. 2020. Available online: https://qgis.org/ (accessed on 17 November 2020).
24. Hargreaves, G.L.; Hargreaves, G.H.; Riley, J.P. Irrigation Water Requirements for Senegal River Basin. *J. Irrig. Drain. Eng.* **1985**, *111*, 265–275. [CrossRef]
25. Hargreaves, G.H.; Allen, R.G. History and Evaluation of Hargreaves Evapotranspiration Equation. *J. Irrig. Drain. Eng.* **2003**, *129*, 53–63. [CrossRef]
26. Vanderlinden, K.; Giráldez, J.V.; Van Meirvenne, M. Spatial Estimation of Reference Evapotranspiration in Andalusia, Spain. *J. Hydrometeorol.* **2008**, *9*, 242–255. [CrossRef]
27. Domínguez-Castro, F.; Santisteban, J.I.; Barriendos, M.; Mediavilla, R. Reconstruction of drought episodes for central Spain from rogation ceremonies recorded at the Toledo Cathedral from 1506 to 1900: A methodological approach. *Glob. Planet. Chang.* **2008**, *63*, 230–242. [CrossRef]
28. Spinoni, J.; Naumann, G.; Vogt, J.V. Pan-European seasonal trends and recent changes of drought frequency and severity. *Glob. Planet. Chang.* **2017**, *148*, 113–130. [CrossRef]
29. Hervás-Gámez, C.; Delgado-Ramos, F. Drought Management Planning Policy: From Europe to Spain. *Sustainability* **2019**, *11*, 1862. [CrossRef]
30. Jiménez-Donaire, M.d.P.; Tarquis, A.; Giráldez, J.V. Evaluation of a combined drought indicator and its potential for agricultural drought prediction in southern Spain. *Nat. Hazards Earth Syst. Sci.* **2020**, *20*, 21–33. [CrossRef]
31. Estrela, T.; Vargas, E. Drought Management Plans in the European Union. The Case of Spain. *Water Resour. Manag.* **2012**, *26*, 1537–1553. [CrossRef]
32. Spinoni, J.; Vogt, J.V.; Naumann, G.; Barbosa, P.; Dosio, A. Will drought events become more frequent and severe in Europe? *Int. J. Climatol.* **2018**, *38*, 1718–1736. [CrossRef]
33. Marcos-Garcia, P.; Lopez-Nicolas, A.; Pulido-Velazquez, M. Combined use of relative drought indices to analyze climate change impact on meteorological and hydrological droughts in a Mediterranean basin. *J. Hydrol.* **2017**, *554*, 292–305. [CrossRef]
34. Gaitán, E.; Monjo, R.; Pórtoles, J.; Pino-Otín, M.R. Impact of climate change on drought in Aragon (NE Spain). *Sci. Total Environ.* **2020**, *740*, 140094. [CrossRef]
35. Wang, J.; Lin, H.; Huang, J.; Jiang, C.; Xie, Y.; Zhou, M. Variations of Drought Tendency, Frequency, and Characteristics and Their Responses to Climate Change under CMIP5 RCP Scenarios in Huai River Basin, China. *Water* **2019**, *11*, 2174. [CrossRef]
36. Sojka, M.; Kozłowski, M.; Kęsicka, B.; Wróżyński, R.; Stasik, R.; Napierała, M.; Jaskuła, J.; Liberacki, D. The Effect of Climate Change on Controlled Drainage Effectiveness in the Context of Groundwater Dynamics, Surface, and Drainage Outflows. Central-Western Poland Case Study. *Agronomy* **2020**, *10*, 625. [CrossRef]

37. Amnuaylojaroen, T.; Chanvichit, P. Projection of near-future climate change and agricultural drought in Mainland Southeast Asia under RCP8.5. *Clim. Chang.* **2019**, *155*, 175–193. [CrossRef]
38. Rosenzweig, C.; Jones, J.W.; Hatfield, J.L.; Ruane, A.C.; Boote, K.J.; Thorburn, P.; Antle, J.M.; Nelson, G.C.; Porter, C.; Janssen, S.; et al. The Agricultural Model Intercomparison and Improvement Project (AgMIP): Protocols and pilot studies. *Agric. For. Meteorol.* **2013**, *170*, 166–182. [CrossRef]
39. Ewert, F.; Rötter, R.P.; Bindi, M.; Webber, H.; Trnka, M.; Kersebaum, K.C.; Olesen, J.E.; van Ittersum, M.K.; Janssen, S.; Rivington, M.; et al. Crop modelling for integrated assessment of risk to food production from climate change. *Environ. Model. Softw.* **2015**, *72*, 287–303. [CrossRef]

CONCLUSIONS

Early and accurate detection and prediction of droughts is crucial for managing agricultural crop production and planning policy response. With this purpose, this study applied two drought indicators and proposed a new combined drought indicator and evaluated the potential of these indicators to detect and predict agricultural droughts, and their relation to crop yield and damage. Overall, this study significantly improved our understanding of agricultural droughts at different spatial and temporal scales.

In chapter 1, the static and dynamic drought stress indicators first proposed by Porporato et al. (2001), have been applied for the first time to evaluate agricultural droughts at local scale (Cordoba province), for the recent period between 2001 and 2014. These indicators, proposed in the framework of ecohydrological research, lack extensive formal validation against independent data, such as crop yield. The results obtained in the present study proved these indicators to be highly useful, as they correctly identified agricultural drought periods in 2005, 2006 and 2012. The results obtained showed that, as predictors of crop yield, both static and dynamic stress indicators are superior to traditional drought indicators such as SPI-3, with R^2 values around 0.70 and 0.40, respectively. A sensitivity analysis revealed that the results were strongly affected by soil depth with a complex response in function of annual precipitation.

In chapter 2, a new combined drought indicator (CDI) was proposed, integrating the well-known SPI-3, the NDVI, and an index of soil moisture anomaly, based on a bucket-type soil moisture model. This CDI was evaluated, at regional scale (Andalusia region), for the recent period between 2003 and 2013, against observed crop damage data in rainfed grain-growing regions. The results show that two important drought events in 2004-2005 and 2011-2012, with crop damage levels of 70 and 95% of the total insured area, respectively, could be identified correctly in the test areas that were used in this study. It was shown that using a combined indicator yielded several advantages over using a single one, as for example soil moisture anomaly alone would not have correctly identified these periods.

In chapter 3, the projected climate change effects on drought events were modelled at national scale (Spain), for the future period between 2006 and 2100. The static and dynamic stress indicators were calculated using predictions of the scenario RCP8.5 in 374 stations. The results showed both the severity and frequency of droughts will increase, especially towards the end of the studied period, 2071-2100. This increase in drought severity and frequency was observed over the whole country, except on the one hand in areas that are already characterized by high stress levels at present, in the southeast of Spain and the Ebro Valley, and on the other hand in areas characterized by no to very low stress, in northern Spain. The results of this study showcased the potential static and dynamic stress indicators, validated in chapter 1. Especially, the dynamic has the advantage, with respect to other indicators, that it includes, besides intensity, information on the mean duration and frequency of drought periods into a single indicator.

Overall, two important conclusions could be drawn from this research, that should be translated into key priorities for future drought management research.

The first main conclusion is that local conditions, namely soil properties and land use type, have a significant impact on the spatial variations of the static and dynamic drought stress indicators, evaluated in chapters 1 and 3; and the Combined Drought Indicator, evaluated in chapter 2. However, soil properties and land use type are rarely considered in evaluations of drought indicators at regional and national scales. Nevertheless, soil properties, especially soil water holding capacity will clearly influence any drought indicator related to soil moisture directly, and any indicator related to vegetation stress indirectly. This importance of local soil properties was explicitly acknowledged in chapter 1, by the sensitivity analysis. These findings corroborates results by Schwantes et al. (2018), who used the same dynamic drought stress indicator to track tree mortality during a 2011 drought in Texas. They found that accounting for the landscape heterogeneity improved greatly the spatial prediction of tree vulnerability to droughts, as accuracy in predicting drought-impacted stands increased from 60%, when they accounted only for spatially variable soil conditions, to 72% when they also included lateral redistribution of water and aspect effects on radiation. Other studies have found contrasting results. Wang et al. (2019) analyzed the spatial variations of the relation between soil moisture and several drought indices in China. They found large spatial variations and concluded that these could be explained by soil properties. They claimed soil bulk density and organic carbon content are the two soil properties most affecting this relation. However, reexamining their data, it can be concluded only soil organic carbon content is significant, as p-values for the relation between soil bulk density and drought indices is always above 0.05. Other soil properties such as texture were not found to be significant either, which is surprising as these affect soil water holding capacity directly. Possibly, this is due to the fact that their database of more than 40 soil moisture stations includes experimental sites with very different land uses, ranging from wheat to complex crop rotations or grasses (Li et al., 2005). Therefore, it can be expected that the type of vegetation, that can be incorporated in regional models by land use category or crop type, will also have a significant impact on the calculated drought indices. Firstly, because vegetation type will directly influence the soil water balance through evapotranspiration and secondly, because of different plant water use strategies and susceptibilities to drought. While different drought indicators exist that allow taking this into account in a more simple or more detailed manner, such as for example the PSDI or CMI, very few studies exist that actually do this in practice at larger spatial scales, from regional-national to continental. One exception is the European Drought Observatory (JRC European Commission, 2020), which also uses a combined drought indicator, comparable to the one used in chapter 2. For the calculation of soil moisture anomaly they rely on LISFLOOD model predictions, which take into account land use and soil properties (Laguardia and Niemeyer, 2008). While this is one off the most advanced models available at this scale, land use is only used to calculate evapotranspiration crop coefficients, not for modulating vegetation susceptibility to drought. Also, soil moisture is not calibrated, and no information on soil depth or rooting

depth is used in the predictions, while our results in chapter 2 showed the importance of this. Therefore, significant progress can be expected when detailed vegetation and soil properties are considered for drought monitoring and prediction.

The second main conclusion is that despite the high volume of drought-related publications, there is still progress to be made in this field, as there are still novel drought indicators with a high potential that have not been widely tested and used. Good examples of this are the static and dynamic drought stress and Combined Drought Index that were proposed here, in chapters 1 and 2, respectively. In any case, it is recommended that the scientific community should increase the testing and validation of existing and new indicators. Keyantash and Dracup (2002) proposed a weighted set of indicators to evaluate drought indicators, including robustness, tractability, transparency, sophistication, extendability, and dimensionality. However, in the case of agricultural droughts, it is more reasonable that validation should be done against independent data from crop yield or crop damage. The amount of studies explicitly validating the performance of drought indicators against such independent data is relatively low, compared to papers evaluating simply occurrence of droughts, as noted by Bachmair et al. (2016). In a revision study, they found that 55 studies evaluated the performance of drought indicators simply against other existing indicators, while only 31 studies evaluated against some form of independent data. Of the latter category, only 14 studies validated against crop yield data. It can be expected that future advances in data availability and big data should make it easier to make this link, as yield variability is already being linked to other agronomic variables (Filippi et al., 2019; van Klompenburg et al., 2020).

References

Bachmair, S., Stahl, K., Collins, K., Hannaford, J., Acreman, M., Svoboda, M., Knutson, C., Smith, K.H., Wall, N., Fuchs, B., Crossman, N.D., Overton, I.C., 2016. Drought indicators revisited: the need for a wider consideration of environment and society. WIREs Water 3, 516–536. https://doi.org/10.1002/wat2.1154

Filippi, P., Jones, E.J., Wimalathunge, N.S., Somarathna, P.D.S.N., Pozza, L.E., Ugbaje, S.U., Jephcott, T.G., Paterson, S.E., Whelan, B.M., Bishop, T.F.A., 2019. An approach to forecast grain crop yield using multi-layered, multi-farm data sets and machine learning. Precis. Agric. 20, 1015–1029. https://doi.org/10.1007/s11119-018-09628-4

JRC European Commission, 2020. European Drought Observatory [WWW Document]. URL https://edo.jrc.ec.europa.eu/edov2/php/index.php?id=1000 (accessed 10.23.20).

Keyantash, J., Dracup, J.A., 2002. The Quantification of Drought: An Evaluation of Drought Indices. Bull. Am. Meteorol. Soc. 83, 1167–1180. https://doi.org/10.1175/1520-0477-83.8.1167

Laguardia, G., Niemeyer, S., 2008. On the comparison between the LISFLOOD modelled and the ERS/SCAT derived soil moisture estimates. Hydrol. Earth Syst. Sci. 12, 1339–1351. https://doi.org/10.5194/hess-12-1339-2008

Li, H., Robock, A., Liu, S., Mo, X., Viterbo, P., 2005. Evaluation of Reanalysis Soil Moisture Simulations Using Updated Chinese Soil Moisture Observations. J. Hydrometeorol. 6, 180–193. https://doi.org/10.1175/JHM416.1

Porporato, A., Laio, F., Ridolfi, L., Rodriguez-Iturbe, I., 2001. Plants in water-controlled ecosystems: active role in hydrologic processes and response to water stress: III. Vegetation water stress. Adv. Water Resour. 24, 725–744. https://doi.org/10.1016/S0309-1708(01)00006-9

Schwantes, A.M., Parolari, A.J., Swenson, J.J., Johnson, D.M., Domec, J.-C., Jackson, R.B., Pelak, N., Porporato, A., 2018. Accounting for landscape heterogeneity improves spatial predictions of tree vulnerability to drought. New Phytol. 220, 132–146. https://doi.org/10.1111/nph.15274

van Klompenburg, T., Kassahun, A., Catal, C., 2020. Crop yield prediction using machine learning: A systematic literature review. Comput. Electron. Agric. 177, 105709. https://doi.org/10.1016/j.compag.2020.105709

Wang, J., Lin, H., Huang, J., Jiang, C., Xie, Y., Zhou, M., 2019. Variations of Drought Tendency, Frequency, and Characteristics and Their Responses to Climate Change under CMIP5 RCP Scenarios in Huai River Basin, China. Water 11, 2174. https://doi.org/10.3390/w11102174